Annual report for the

Norwegian National Seismic Network

2015

Supported by

University of Bergen

and

Norwegian Oil and Gas Association

Prepared by

Department of Earth Science
University of Bergen
Allegaten 41, N-5007 Bergen

April 2016

CONTENTS

1 Introduction

This annual report for the Norwegian National Seismic Network (NNSN) covers operational aspects for the seismic stations contributing data, presents the seismic activity in the target areas and the associated scientific work carried out under the project. The report is prepared by the University of Bergen with contributions from NORSAR.

The NNSN network is supported by the oil industry through the Norwegian Oil and Gas Association and the University of Bergen (UiB).

1.1 Data availability to the public

All the data stored in the NNSN database are available to the public via Internet, e-mail or on manual request. The main web-portal for earthquake information is www.skjelv.no. It is possible to search interactively for specific data and then download the data from ftp://ftp.geo.uib.no/pub/seismo/DATA. Data are processed as soon as possible and updated lists of events recorded by Norwegian stations are available soon after recording. These pages are automatically updated with regular intervals.

2 Operation

2.1 NNSN

The University of Bergen (UiB) has the main responsibility to run the NNSN and operates 33 of the seismic stations that form the NNSN located as seen in Figure 1. NORSAR operates 3 seismic arrays, which also include broadband instruments, and three single seismometer stations (JETT, JMIC and AKN).

In addition to the NNSN stations, waveform data from other selected stations in Finland (University of Helsinki), Denmark (GEUS), Sweden (University of Uppsala) and Great Britain (BGS) are transferred in real time and included in the NNSN database. More than 20 stations located in or operated by neighbouring countries are recorded continuously in Bergen and can be used for locating earthquakes, see Figure 1 and Figure 2. Phase data from arrays in Russia (Apatity), Finland (Finess), Sweden (Hagfors) and stations operated by the British Geological Survey (BGS) are also included when available.

The seismicity detected by the network is processed at UiB, however NORSAR also integrates their results in the joint database at UiB. In total, NORSAR provides data from 12 broadband stations to the NNSN. One station with real-time data is provided from the Ekofisk field by ConocoPhillips. The station HSPB is operated jointly between NORSAR and the Geophysical Institute, Polish Academy of Sciences, Warsaw, Poland and the stations BRBA and BRBB are a collaboration between NORSAR and the Kola Science Centre, Russian Academy of Sciences, Apatity, Russia. BRBA and BRBB are both located in Barentsburg, Svalbard.

At NORSAR the parameters of analyst-reviewed events are converted into parameter files in Nordic format and forwarded via ftp to UiB on a daily basis. The magnitude threshold is set to about M 1.5 for regional events of potential interest for the NNSN. After transferring the parameter files, the NORSAR analyst logs into the the UiB database using SEISAN and integrates the events. Integration means to merge NORSAR and UiB events, which may require to repick seismic phases, to include new phase readings, to edit double phase readings and to relocate the seismic event with the new parameters.

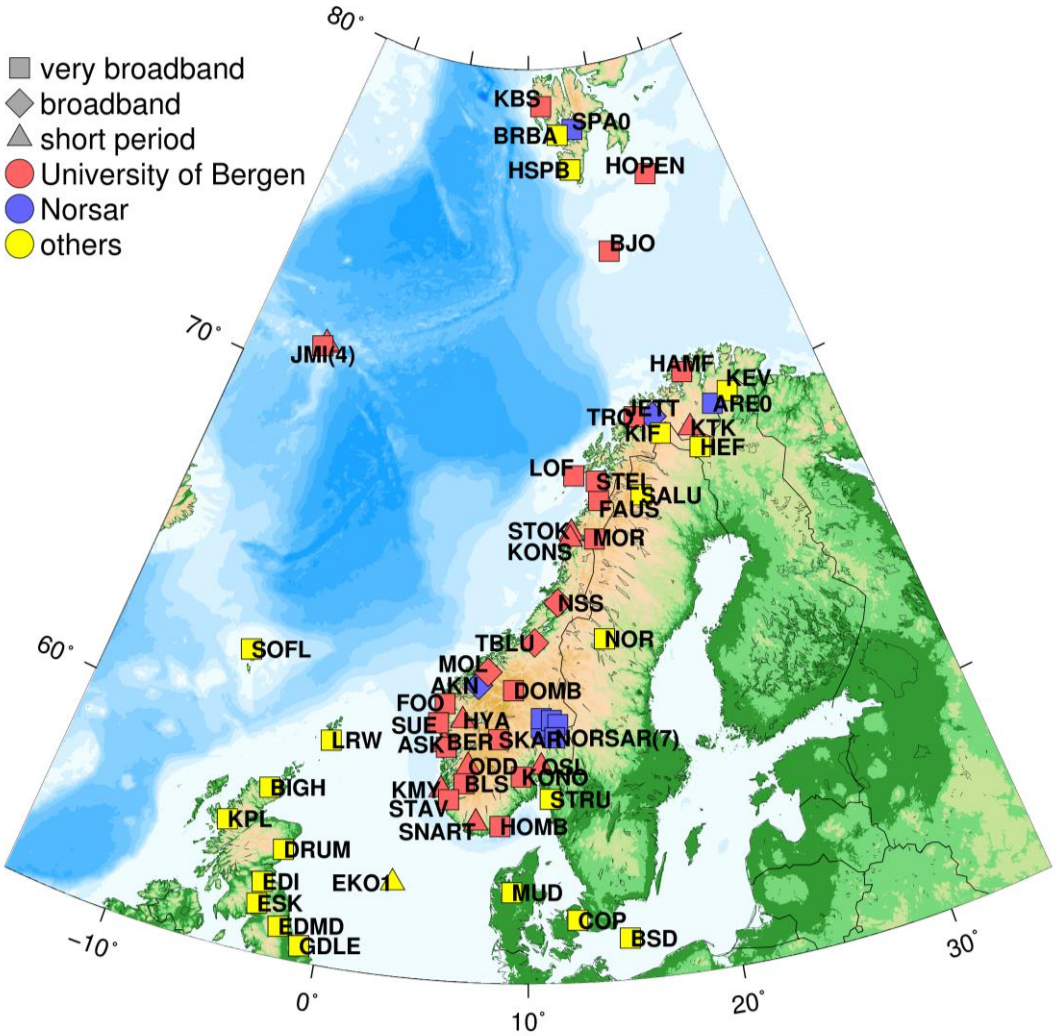

Figure 1. Stations contributing to the Norwegian National Seismic network (NNSN). UiB operates 33 stations (red) and NORSAR operates the stations marked in blue, including the three arrays and stations AKN and JMIC.

Seismic data recorded at stations located on Greenland and operated by GEUS are included in the NNSN real-time processing, Figure 2. These data are important for the location of earthquakes west of Jan Mayen and at the northern part of the Knipovich ridge to the Gakkel ridge.

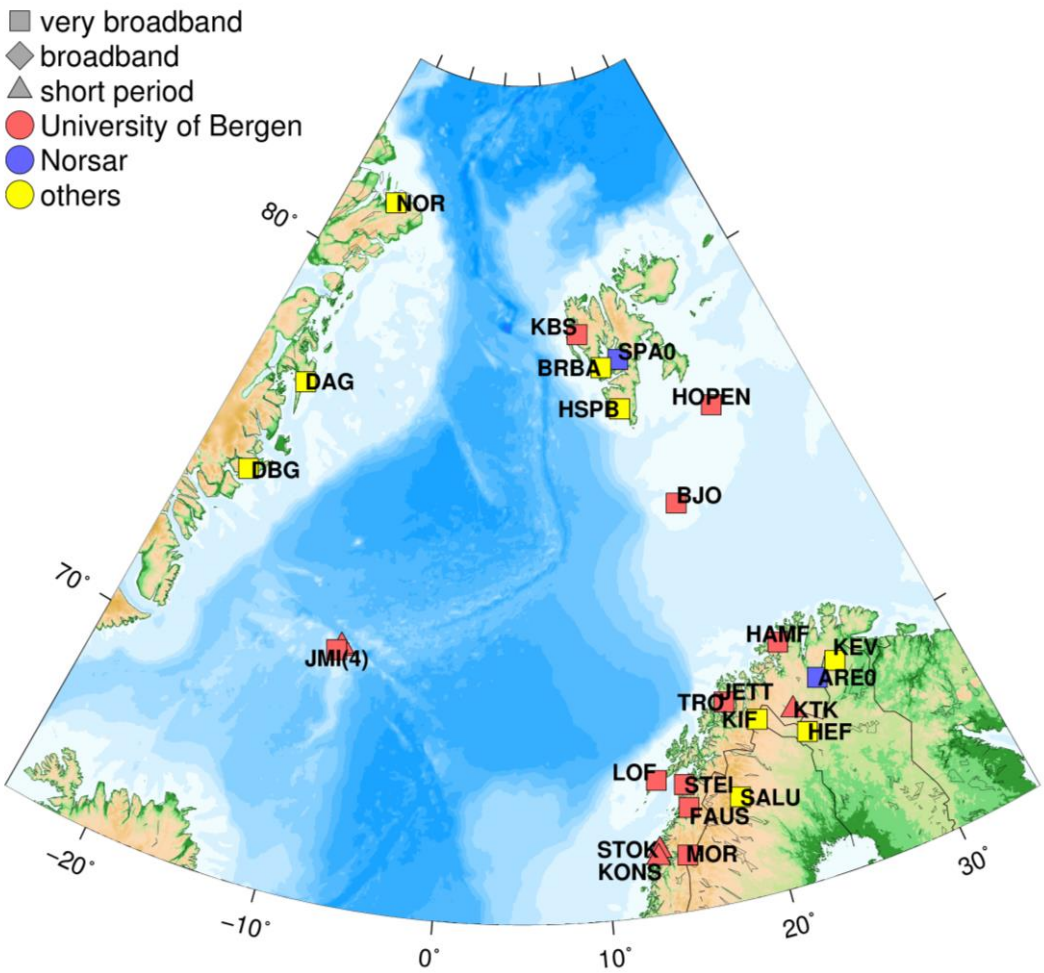

Figure 2. Seismic stations in the arctic area.

UiB is in the process of upgrading the NNSN by changing short period (SP) to broadband (BB) seismometers. A further effort is made to install additional high quality digitizers. The current status of this upgrade is shown in Table 1. As of today the numbers of SP, BB stations and stations with real time transmission are listed in Table 1.

Table 1. Overview of UiB seismic stations

	Short Period	Broadband	Real time
Number of stations	10	23 (20 with natural period greater than 100 sec)	30 (not real time are 2 short period and 1 broadband stations on Jan Mayen)

The operational stability for each station is shown in Table 2. The down time is computed from the amount of data that are missing from the continuous recordings at UiB. The statistics will, therefore, also show when a single component is not working. This is done as the goal is to obtain as complete continuous data from all stations as possible. Also, communication or

computing problems at the centre will contribute to the overall downtime. In the case of communication problems, a station may not participate in the earthquake detection process, but the data can be used when it has been transferred. Thus, the statistics given allow us to evaluate the data availability when rerunning the earthquake detection not in real-time.

The data completeness for the majority of the stations is above 95%, except for the following stations KONS, MOR8 and TBLU (see technical service overview for details).

Table 2. Data completeness in % for 2015 for all stations of the NNSN operated by UiB.

Station	Data completeness %		Station	Data completeness %
Askøy (ASK)	95		Kings Bay (KBS)	99
Bergen (BER)	100		Kongsberg (KONO)	99
Bjørnøya (BJO)	99		Konsvik (KONS)	90
Blåsjø (BLS)	99		Lofoten (LOF)	99
Dombås (DOMB)	100		Mo i Rana (MOR8)	88
Fauske (FAUS)	100		Molde (MOL)	97
Florø (FOO)	96		Namsos (NSS)	100
Hammerfest (HAMF)	100		Odda (OOD1)	95
Homborsund (HOMB)	100		Oslo (OSL)	100
Hopen (HOPEN)	98		Skarslia (SKAR)	100
Høyanger (HYA)	98		Snartemo (SNART)	100
Jan Mayen (JMI)	99		Stavanger (STAV)	99
Jan Mayen (JNE)	99		Steigen (STEI)	99
Jan Mayen (JNW)	99		Stokkvågen (STOK)	99
Karmøy (KMY)	100		Sulen (SUE)	98
Kautokeino (KTK1)	98		Blussuvoll (TBLU)	69
			Tromsø (TRO)	97

2.2 The NORSAR stations and arrays

The NNSN uses selected data (as stated above) from the NORSAR installations that are funded outside the NNSN project.

NORSAR is operating the following seismic installations in Norway:

- NOA (southern Norway, array, 42 sites, 7 3C broadband sensors and 35 vertical broadband sensors)
- ARCES (Finmark, array, 25 sites, 25 3C broadband seismic sensors 80 Hz)
- SPITS (Spitsbergen, array, 9 sites, 6 3C broadband sensors and 3 vertical broadband sensors)
- NORES (Hedmark, array, 9 3C short-period sensors, 9 infrasound sensors)
- JMIC (Jan Mayen, 3C broadband sensor)
- AKN (Åknes, Møre og Romsdal, 3C broadband sensor)
- JETT (Jettan, Troms, 3C broadband sensor)

In addition NORSAR receives and processes data in near realtime from:

- FINES (southern Finland, array, 16 sites, 2 3C broadband sensor, 1 3C short-period sensor and 15 short-period vertical sensors, operated by Institute of Seismology, Helsinki, Finland)
- HFS (Hagfors, Sweden, 10 sites, 1 3C broadband sensor and 9 short-period vertical sensors, operated by the Swedish Defence Research Agency, Stockholm, Sweden)
- EKA (Eskdalemuir, United Kingdom, 20 sites, 1 3C broadband sensor and 20 short-period vertical sensors, operated by the United Kingdom National Data Centre, AWE Blacknest, UK)

The seismic array data are automatically processed and analysed. The fastest near realtime process 'Automatic Alert' is based on single array detection and provides event locations within a few (1-3) minutes delay. The alerts with event and location details are published immediately on http://www.norsardata.no/NDC/ael/eventmap1.html (which is also integrated into the NNSN website). A second automatic process called GBF (Generalized Beam Forming) awaits for automatic phase picks from all arrays and delivers more reliable/accurate results within up to a few hours delay. Automatically processed seismic events with magnitude larger than 2 (or 1.5 if the event is of special interest) are manually analysed and reviewed. In this step all available waveforms (also from single stations) are utilized. Graphical displays and parametric event data and for 'Automatic Alert', 'GBF' and 'Reviewed bulletins' can be found on http://www.norsardata.no/NDC/bulletins/.

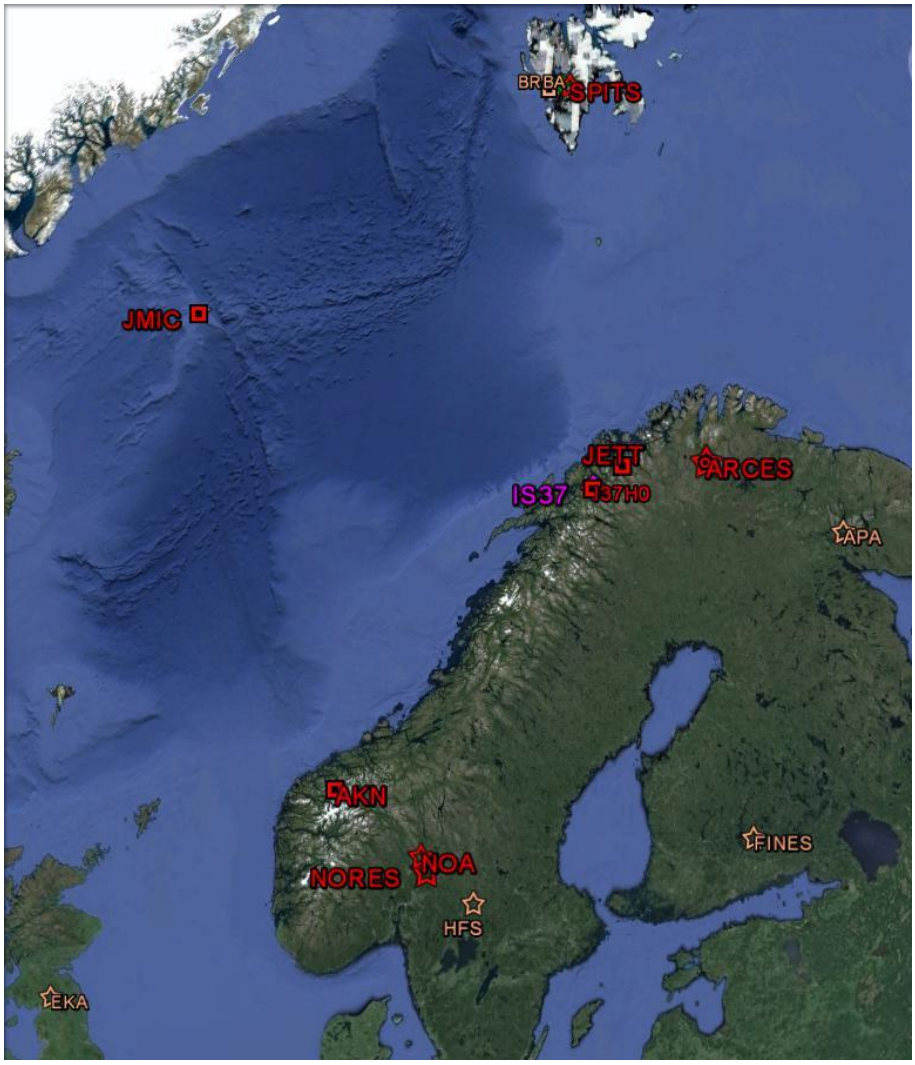

Figure 3 NORSAR seismic arrays/stations (NOA, NORES, ARCES, SPITS, JMIC, AKN, I37H0) and contributing arrays/stations (HFS, FINES, EKA, BRBA, APA).

All data recorded at NORSAR are continuous. The following table provides a monthly overview on the data availability of 13 main data streams provided by NORSAR to NNSN.

Table 3. Systems recording performance (in % of data completeness) for 14 main data streams provided from NORSAR to NNSN.

	ARA0	JMIC	NAO01	NBO00	NB201	NC204	NC303
Jan	99.97	99.88	99.96	99.97	99.95	99.97	99.97
Feb	100.00	99.99	99.98	99.98	99.98	99.96	89.86
Mar	100.00	100.00	100.00	99.99	100.00	100.00	100.00
Apr	100.00	99.99	100.00	100.00	99.99	100.00	100.00
May	100.00	85.71	99.99	99.97	94.36	99.99	100.00
Jun	100.00	99.94	99.98	99.98	99.97	99.99	99.97
Jul	100.00	99.49	99.96	100.00	100.00	99.99	100.00
Aug	99.99	99.81	99.85	100.00	100.00	100.00	99.99
Sep	95.48	99.96	99.95	100.00	100.00	100.00	100.00
Oct	99.99	100.00	99.87	100.00	100.00	100.00	99.99
Nov	99.99	99.91	99.90	99.78	100.00	99.99	99.99
Dec	100.00	100.00	99.89	99.98	100.00	100.00	100.00

	NC405	NC602	SPA0	AKN	JETT	HFC2	I37H0
Jan	99.97	99.98	88.43	99.99	100.00	74.53	-
Feb	99.98	100.00	94.40	100.00	100.00	100.00	-
Mar	100.00	100.00	95.41	100.00	100.00	99.99	-
Apr	100.00	100.00	100.00	100.00	100.00	96.60	-
May	100.00	99.74	97.91	100.00	100.00	100.00	-
Jun	99.95	100.00	100.00	100.00	100.00	100.00	-
Jul	99.96	100.00	99.99	100.00	100.00	99.98	64.52
Aug	99.99	100.00	99.78	99.99	99.72	97.57	99.85
Sep	100.00	100.00	99.96	99.53	99.99	100.00	99.97
Oct	99.99	100.00	100.00	97.65	100.00	99.19	100.00
Nov	99.99	100.00	100.00	100.00	100.00	99.99	100.00
Dec	99.99	100.00	100.00	100.00	100.00	99.99	99.99

The NORSAR analysis results are based on automatic phase detection and automatic phase associations which produce the automatic bulletin. Based on the automatic bulletin a manual analysis of the data is done, resulting in the reviewed bulletin. The automatic bulletin for northern Europe is created using the Generalized Beam Forming (GBF) method. This bulletin (www.norsardata.no/NDC/bulletins/gbf/) is subsequently screened for local and regional events of interest in Fennoscadia and in Norway, which in turn are reviewed by an analyst. Regional reviewed bulletins from NORSAR are available from 1989 and from 1998 onwards they are directly accessible from via internet (www.norsardata.no/NDC/bulletins/regional/). Table 4 gives a summary of the phase detections and events declared by GBF and the analyst.

Table 4. Phase detections and event summary.

	Jan.	Feb.	March	April	May	June
Phase detections	158549	155398	183846	150223	161062	177784
Associated phases	5827	4783	5316	4913	5416	6151
Un-associated phases	152722	150615	178530	145310	155646	171633
Screened GBF events for Fennoscandia/Norway	1171	890	996	817	977	1238
No. of events defined by the analyst	62	32	51	52	45	49
	July	**Aug.**	**Sep.**	**October**	**Nov.**	**Dec.**
Phase detections	205692	212534	267323	273975	238272	242688
Associated phases	6906	8984	13740	14916	11299	12076
Un-associated phases	198786	203550	253583	259059	226973	230612
Screened GBF events for Fennoscandia/Norway	1577	2139	3297	3486	2452	2557
No. of events defined by the analyst	64	55	41	40	56	58

Changes to the NORSAR arrarys:

- The NORES array was upgraded from three-component short-period to three-component broadband mid of August 2015 (13.8.2015).
- A 3C Guralp broadband sensor was added into the central pit of the infrasound array I37NO in Bardufoss.
- All 9 digitizers of the SPITS array were replaced.

2.3 Field stations and technical service NNSN

The technical changes for each seismic station are listed below. It is noted if these changes are carried out by the respective local contact and not by the technical staff of UiB. When a station stops working, tests are made to locate the problem. Sometimes the reason cannot be found and the cause of the problem will be marked as unknown.

Major changes during this reporting period of 2015 were:

Ask (ASK)	07.01.15: Visit. Malfunctioning digitizer is replaced. The station down from 20. December 2014 and data is lost.
	20.01.15: Visit: Station was down due to lightning. Changed digitizer, GPS-antenna, power supply. Industrial-PC phased out. Removed remains from older installations.
	22.01.15: Visit. Changed GSM router. Inspection of earth grounding rod and measurement of its resistivity. Checked station coordinates.
	26.10.15: Visit. Changed GSM router with ICE version.
Bergen (BER)	03.02.15: In order to test the STS-2 sensor that was phased out at HOPEN in Sept 2014, we swapped the BER STS-2 unit with the one from HOPEN. Testing started Tue Feb 3. 2015 and was completed Thu 5 Feb., when the original BER STS-2 sensor was put into operation again
Bjørnøya (BJO1)	21.08.15: Visit. Inspection. The digitizer was moved to sensor, GPS antenna installed on nearby pole and mass centered.
	08.10.15: Local personnel replaced Ethernet Extender unit in sensor box with a spare unit.
Blåsjø (BLS)	04.12.15: Station down since 20.11.15 due to problems with the internet line (fiber cable). PC removed, now Guralp digitizer installed. The fiber modem replaced with media converter (fiber->Ethernet) and a Zyxel router.
Blussvoll (TBLU)	10.03.15: Visit. PC and power supply replaced.
	24.03.15: Visit. Replaced serial cable between sensor and recording equipment. Data lost since February 18. Discussed possible new site with Stjørdal Kommune.

	17.08.15: Local contact installed new industrial PC. Data lost since June 24.
	21.09.15: PC problem. Local contact installed and tested SMS reset device. Replaced industrial PC with new unit.
Dombås (DOMB)	27.11.15. New ICE-router installed by local contact.
Fauske (FAUS)	04.03.15: Local operator. Water, possibly caused by condensation, was removed from the vault. A new lid and gasket were installed to avoid condensation.
	13.03.15: Local operator. New cable installed between router and digitizer.
	25.05.15: Local operator. Water removed, attempt to install new router which did not work so the old router was reinstalled. Switched back to the original network cable between router and digitizer.
	11.06.15: Visit. Changed digitizer and router.
	17.06.15. Communication down since 1. june. The router operated by default in 4G, but FAUS is outside 4G area. Parameter settings changed on router.
	12.09.15: Replaced lid. Work done by local entrepreneur.
	16.10.15: Visit for inspection and maintenance.
	30.10.15: Padlock, pressure-proof entry and tube installed by local operator.
	01.11.15. Adapter installed by local contact.
Florø (FOO)	11.03.15: Visit. Replaced the digitizer and power supply.
Hammerfest (HAMF)	No visit or technical changes.
Homborsund (HOMB)	No visit or technical changes
Hopen (HOPEN)	26.08.15: Visit. New vault installed. New installation of seismometer, digitizer and telemetry between building and vault.
	21.09.15: Local staff at Hopen finished the backfilling and the remaining el. work.
	15.10.15: During October the local staff at Hopen did minor maintenance.
Høyanger (HYA)	30.12.15. Short power loss. Restarted the power using sms.
Jan Mayen (JMI)	17.10.15: Inspection by local operator.
JNE	Inspected by local operator. No technical changes.

JNW	Inspected by local operator. No technical changes.
Karmøy (KMY)	18.12.15. Communication down from 13.12 to 17.12. A GSM-Mini restart is installed. No data lost.
Kautokeino (KTK)	14.07.15: Visit. Replaced the ranger seismometer with a Streckeisen STS-2.5 on loan from Norwegian broadband pool until end of 2016. 24.07.15: Masscentering done by local contact. 31.07.15: Local contact checked the sensor. No mass-centering needed. 24.11.15: Station down since 18.11 due to broken digitizer. New digitizer installed by local operator. All data from this timeperiod is lost.
Kings Bay (KBS)	No visit or technical changes.
Kongsberg (KONO)	No visit or technical changes.
Konsvik (KONS)	25.03.15: Station down until April 07. 2015 because of power-loss during the Easter vacation. Data lost. 18.05.15: PC problem. The local contact absent May 5-12. New PC installed. Data lost between April 28- May 18.
Lofoten (LOF)	No visit or technical changes.
Mo i Rana (MOR8)	04.03.15: Station has been down since February 07. 2015 due to a faulty PC. The PC has been replaced. Data has been lost. 21.07.15: Station down from July 19. Resetting of power supply and digitizer done remotely.
Molde (MOL)	17.02.15: Power loss due to lightning. New sensor installed, COM 1 and 2 on the industrial PC was defect, but COM 3 and 4 could be used. Data lost.
Namsos (NSS)	No visit or technical changes.
Odda (ODD1)	10.09.15: The PC was defect. New PC and modem were shipped to the local contact. Due to holiday the new PC and modem was installed 11th September. Data is lost between August 28 and September 10.
Oslo (OSL)	18.09.15: Visit. Installed new Nanometrics interface cable between digitizer (Güralp DM24-EAM) and sensor (Nanometrics Trillium 120PA). Phased out old cable with two junction boxes.
Skarslia (SKAR)	12.07.15: Visit. Inspection. 08.10.15: Visit. Inspection.

Snartemo (SNART)	No visit or technical changes.
Stavanger (STAV)	05.01.15: Station down until January 07. 2015 due to power break at OD. Data lost.
Steigen (STEI)	No visit or technical changes.
Stokkvågen (STOK)	No visit or technical changes.
Sulen (SUE)	20.11.15: Remote restart of GSM-router. Station down some hours. No data lost.
Tromsø (TRO)	14.04.15: Station has been down from April 04.04. 2015 due to a defective PC. PC has been replaced by local operator. Data lost.
Vadsø (VADS)	16.10.15: Visit. The vault for the new station was constructed

3 NNSN achievements and plans

The overall purpose of the NNSN is to provide data both for scientific studies, but equally important for the routine observation of earthquakes. This in principle means that broadband seismometers are desired at all sites. However, in areas where additional stations are deployed for local monitoring, short-period seismometers are sufficient. The number of broadband seismometers in the network will be increased to replace existing short period instruments. A general goal for the future development has to be to achieve better standardization in particular with the seismometers and digitizers. The total number of stations for now should remain stable, but it is important to improve the overall network performance.

3.1 NNSN achievements in 2015

- Two EPOS proposals have been approved, the first (EPOS-IP) will allow UiB to lead IT developments on data and service integration at the European scale; the second (EPOS-N) is funded by the Norwegian Research Council to install new monitoring stations in Northern Norway and the Arctic as well as develop tools for processing and visualization, and provide the different geo-scientific data through a web-portal.
- Hopen: The seismic station was re-built with a new vault and equipment. The digitizer is now placed at the vault.
- Bjørnøya (BJO): The station was improved by moving digitizer to the sensor vault.

- OSL, BJO, HOPEN, SKAR : New cabling to connect the Nanometrics sensor to Guralp digitizer without junction boxes has been implemented at a number of sites
- The new station near Vadsø (VADS) on the Varanger peninsula is under construction.
- The KTK station has been temporarily upgraded with a broadband seismometer on loan from the Norwegian broadband pool.
- Initiate the plans for finding new site for station TBLU (Trondheim). The local authority in Stjørdal, north of Trondheim, has been contacted to find a possible site for noise measurements.
- The manuscript on the seismic noise analysis and interpretation is accepted for publication in Journal of Seismology.
- The research work at UiB this year was carried out by two guest researchers, Won-Young Kim (Columbia University) and Luigia Cristiano (Kiel University), during the fall, where the focus is on polarization analysis and development of magnitude scales in particular to address the complicated travel paths in the North Atlantic not accounted for in the current magnitude scale. The work is presented in section 5.The research work by NORSAR on travel time inversion is giving first results. 3D crustal velocity models for the southern part of Norway and the Nordland region, and Finnmark were developed (see 5.3)
- Spectrogram displays have been implemented at UiB to discriminate between explosion and earthquake. In parallel, NORSAR have implemented a tool to objectively discriminate between earthquakes and explosions, based on a method developed at the Institute of Seismology in Helsinki, Finland and applied it to 2 stations of NNSN (see 5.4).
- NORSAR have relocated earthquakes along the ocean ridges from Jan Mayen to the Gakkel Ridge using NNSN data, together with data from the Danish National Network and global stations.
- A tool (PQLX) to effectively monitor station noise has been implemented and is used routinely.
- The station coordinates have been checked and corrected by comparison to online mapping services. The effect of the correction on earthquake location has been systematically investigated.
- During fall 2015 the Scandinavian countries agreed to get a common classification of recorded events. The classification is continuing and will be finalized during 2016.

3.2 NNSN plans for 2016

- Complete the installation of the new station VADS, planned installation spring 2016.
- Upgrade of two short period stations in south-western Norway with a broadband sensor already purchased in 2015.
- Include the new developed magnitude scales into the routine processing.
- Include the new and improved velocity models for Norway in the routine processing.
- Integrate Statoil data into the real-time processing.
- EPOS: Plan locations for new seismic stations in Nordland and the Artic complementing the existing NNSN stations.
- The research and development activity will continue in close collaboration between UiB and NORSAR.
- Continue collaboration with NORSAR on data processing through technical visits.

- Improve macroseismic questionnaire in collaboration with other Scandinavian countries.
- Improve data exchange:
    - Parametric data from the Icelandic Meteorological Office would increase the location accuracy in the NNSN database for large earthquakes located in the vicinity of Iceland and in the area between Iceland and Jan Mayen. As of today data is available on request.
    - Integrate more real-time continuous data from stations located in Sweden.

3.3 Projects related to NNSN

3.3.1 NEONOR2

The Petromaks funded project NEONOR2 started in 2013 and is a collaboration between NGU, Kartverket, the University of Bergen (UiB), NORSAR, University of Lulea and NPD.
As part of the NEONOR2 project 26 temporary seismic stations were deployed. The locations of the NEONOR2 and the NNSN stations are shown in Figure 4. Data from many of the stations are continuously transferred to Bergen and are used in the daily processing. The stations will remain in the field until spring 2016. The focus of the seismological component of the project has been to compute fault plane solutions and to obtain more precise relative earthquake locations.

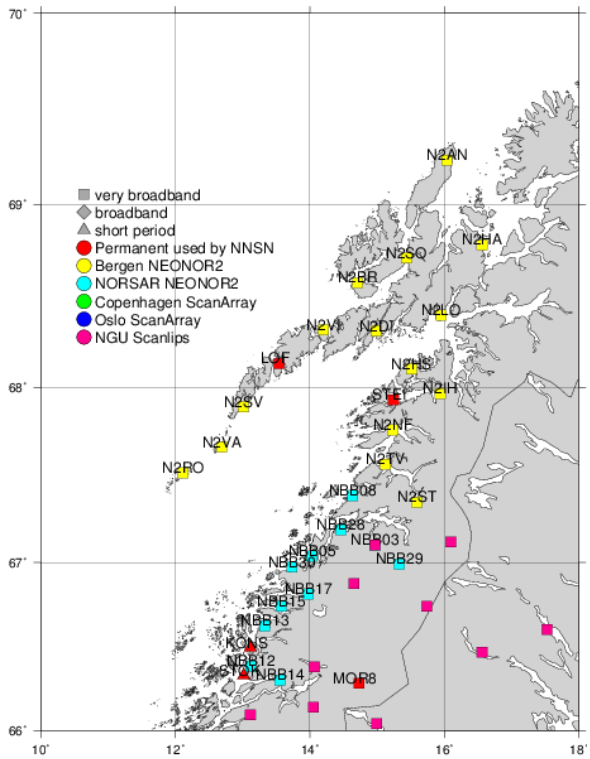

Figure 4. Map of stations deployed in Northern Norway in 2013/2014 and the permanent NNSN

3.3.2 EPOS

The European Plate Observing System (EPOS) has started with its implementation phase in the autumn of 2015 (https://www.epos-ip.org/). EPOS-Norway is funded by the Research Council of Norway (RCN) for five years during the period 2016-2020 and consists of the following six partner institutions:

- Department of Earth Science, University of Bergen (GEO-UiB) - coordinator
- Department of Geosciences, University of Oslo (GEO-UiO)
- Geological Survey of Norway (NGU)
- Stiftelsen NORSAR
- National Mapping Authority (NMA)
- Christian Michelsen Research AS (CMR)

EPOS-Norway has the following three main components:

- Component-1: **Develop a Norwegian EPOS e-infrastructure** to integrate the data from the seismological and geodetic networks, as well as the data from the geological and geophysical data repositories, which is in line with European EPOS.
- Component-2: **Improved monitoring capacity in the Arctic**, including northern Norway and the Arctic islands.
- Component-3: **Establish a Solid Earth Science Forum** for providing a constant feedback mechanism for improved integration of multidisciplinary data, as well as training of young scientists for future utilization of all available solid Earth observational data through a single e-infrastructure.

Improved monitoring in the Arctic involves installation of seismological and geodetic stations on Svalbard (6 new installations), Bjørnøya (new 9-component array), Jan Mayen (2 upgrades and 1 new installations) and Northern Norway (7 new installations).

4 Seismicity of Norway and surrounding areas for 2015

The earthquake locations presented have been compiled from all available seismic stations as described above. All phase data are collected by UiB, and a monthly bulletin is prepared and distributed. All local and regional earthquakes recorded on NNSN stations are presented on the web pages and the largest are also e-mailed to the European-Mediterranean Seismological Centre (EMSC) to be published on the EMSC web pages. A brief overview of the events published in the monthly bulletins is given in this annual report. Macroseismic data for the largest felt earthquakes in Norway are collected, and macroseismic maps are presented.

Local, regional and teleseismic events that are detected by the UiB network are included. The merging of data between NORSAR and UiB is based on the following principles:

i) All local and regional events recorded by NORSAR that are also detected by the NNSN network are included.

ii) All local and regional events with local magnitude larger than 1.5 detected by NORSAR and not recorded by the NNSN are included.

iii) All teleseismic events recorded by NORSAR and also detected by the NNSN are included.

iv) All teleseismic events with NORSAR magnitude $M_b \geq 5.0$ are included even not detected by the NNSN.

Data from the British Geological Survey (BGS) and the Geological Survey of Denmark and Greenland (GEUS) are included in the database in Bergen following similar criteria as mentioned above, however only events located in the prime area of interest, 54-82°N and 15°W-35°E, and with magnitude ≥ 2.0 are included. Identified earthquakes located in northern Scandinavia, are routinely e-mailed from University of Helsinki and included in the NNSN database following the principles above.

Many of the recorded events are explosions. To discriminate between natural earthquakes and manmade explosions the spectrograms are studied. This was introduced after a visit by the processing staff to the University of Helsinki in November 2014, and implemented in the processing in Bergen during spring 2015.

4.1 Velocity models and magnitude relations

The velocity model used for locating all local and regional events, except for the local Jan Mayen events, is shown in Table 5 (Havskov and Bungum, 1987). Event locations are performed using the HYPOCENTER program (Lienert and Havskov, 1995) and all processing is performed using the SEISAN data analysis software (Havskov and Ottemöller, 1999).

Table 5. Velocity model used for locating all local and regional events, except for the local Jan Mayen events (Havskov and Bungum, 1987).

P-wave velocity (km/sec)	Depth to layer interface (km)
6.2	0.0
6.6	12.0
7.1	23.0
8.05	31.0
8.25	50.0
8.5	80.0

Magnitudes are calculated from coda duration, amplitudes or displacement source spectra. The coda magnitude relation was revised in 2006 (Havskov & Sørensen 2006). The coda wave magnitude scale (M_C) is estimated through the relation

$$M_C = -4.28 + 3.16 \cdot \log10(T) + 0.0003 \cdot D$$

where T is the coda length in seconds and D is the epicentral distance in km. The new scale made M_C more consistent with M_L since M_C in general is reduced. For this report all data are updated using the new magnitude scale. When instrument corrected ground amplitudes A (nm) are available, local magnitude M_L is calculated using the equation given by Alsaker et al. (1991):

$$M_L = 1.0 \cdot \log(A) + 0.91 \cdot \log(D) + 0.00087 \cdot D - 1.67$$

where D is the hypocentral distance in km.

The moment magnitude M_w is calculated from the seismic moment M_0 using the relation (Kanamori, 1977)

$$M_w = 0.67 \cdot \log(M_0) - 6.06$$

The unit of M_0 is Nm. The seismic moment is calculated from standard spectral analysis assuming the Brune model (Brune, 1970) and using the following parameters:

Density: 3.0 g/cm^2
$Q = 440 \cdot f^{0.7}$
P-velocity = 6.2 km/s
S velocity = 3.6 km/s

For more computational details, see Havskov and Ottemöller, (2003).

For the Jan Mayen area, a local velocity model (see Table 6) and coda magnitude scale is used (Andersen, 1987).

Table 6. Velocity model used for locating local Jan Mayen events.

P-wave velocity (km/sec)	Depth to layer interface (km)
6.33	18
8.25	50

The coda magnitude scale for Jan Mayen which is used in this report is given by Havskov & Sørensen (2006). This scale was implemented in 2006 but all events used in this report are updated during April/May 2006.

$$M_C = 3.27 \cdot \log(T)\ 2.74 + 0.001 \cdot D$$

where T is the coda duration and D is the epicentral distance in km.

The regional and teleseismic events recorded by the network are located using the global velocity model IASPEI91 (Kennett and Engdahl, 1991).

Body wave magnitude is calculated using the equation by Veith and Clawson (1972):

$$Mb = \log(A/T) + Q(D,h)$$

Here h is the hypocentre depth (km), A is the amplitude (microns), T is period in seconds and Q(D,h) is a correction for distance and depth.

Surface wave magnitude Ms is calculated using the equation (Karnik et al., 1962):

$$Ms = \log(A/T) + 1.66 \cdot \log(D) + 3.3$$

where A is the amplitude (microns), T is period in seconds and D is the hypocentral distance in degrees.

Starting from January 2001, the European Macroseismic Scale, EMS98, (Grünthal, 1998) has been used. All macroseismic intensities mentioned in the text will refer to the EMS98 instead of the previously used Modified Mercalli Intensity scale. The two scales are very similar at the lower end of the scale for intensities less than VII.

4.2 Events recorded by the NNSN

Based on the criteria mentioned in section 4, a total of 6,833 local and regional events, were detected by the NNSN during 2015. Of these local and regional events, 39% were large enough to be recorded by several stations and hence could be located reliably, and are not classified as explosions (LP or LE). The numbers of local/regional and teleseismic events, recorded per month in 2015 are shown in Figure 5. The average number of local and regional events recorded per month is 570.

A total of 1101 teleseismic events were recorded in 2015 and the monthly average of teleseismic earthquakes in the NNSN database, is 91. In addition to the locations determined at UiB and NORSAR, also preliminary locations published by the USGS (United States Geological Survey) or the EMSC (European Mediterranean Seismological Centre) based on the worldwide network are included for earthquakes also registered by NNSN stations.

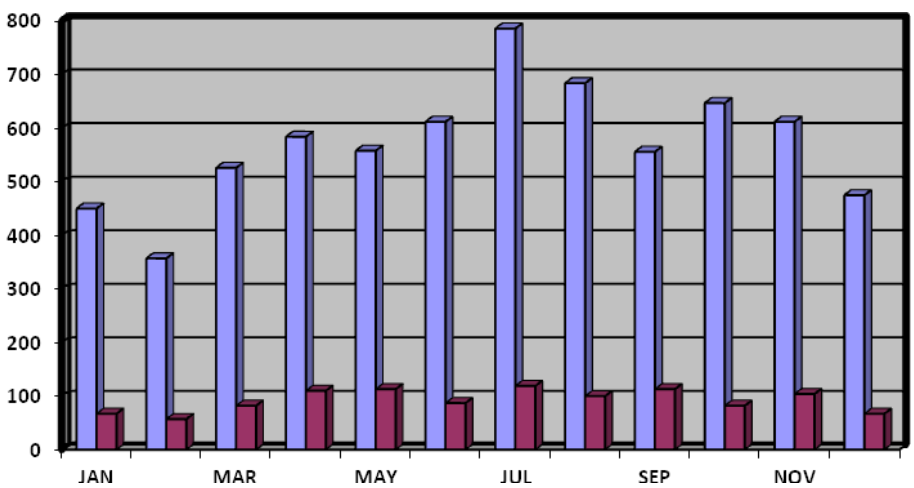

Figure 5. Monthly distribution of local/regional and distant events, recorded during 2015.

UiB, as an observatory in the global network of seismological observatories, reports local and teleseismic phases to the International Seismological Center (ISC). All events (teleseismic, regional and local) recorded from January to December 2015 with M ≥ 3 are plotted in Figure 6.

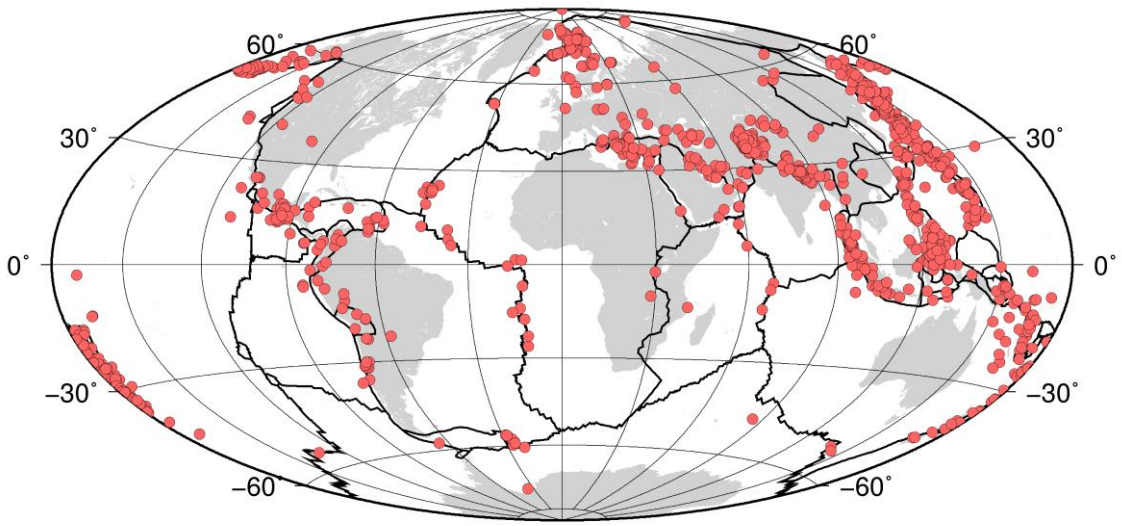

Figure 6. Epicentre distribution of earthquakes with M≥3.0, located by the NNSN from January to December 2015. Teleseismic events recorded only by NORSAR have M≥5.0.

Monthly station recording statistics from January to December 2015 are given in Table 6 and 7. This table shows, for each station, local events recorded on more than one station and recorded teleseismic events. The statistics are based on the analysed data and are taken from the database. Table 6 and 7 show both earthquakes and explosions. Identified or suspected explosions will only be located with a minimum number of stations. Therefor some stations (e.g. KTK, MOR8) will have a higher number of detections.

The following was observed from Table 6 and 7:

- At Jan Mayen there was an increase in earthquake activity during June and July.
- The number of local earthquakes recorded at HOPEN (and for some months also BJO) is higher than expected when compared to 2014.
- TBLU and OSL are recording mostly teleseismic earthquakes, which is as expected due to their location in noisy environment. Stronger local earthquakes will however be detected.
- TBLU was down a period during summer 2015 due to PC problems.
- The stations KONS, STOK and MOR8 continue to record a relatively large number of small earthquakes and explosions in the area. Temporary stations were deployed during fall 2013 and an increase in smaller events recorded and located in this area is expected during the NEONOR2 project period.

Table 7. Monthly statistics of events recorded at each station for January-June 2015. Abbreviations are: L = Number of local events recorded at more than one station and D = Number of teleseismic events recorded at the station.

	JANUARY		FEBRUARY		MARCH		APRIL		MAY		JUNE	
STATION	**L**	**D**	**L**	**D**	**L**	**D**	**L**	**D**	**L**	**D**	**L**	**D**
ASK	11	13	35	23	65	19	46	32	30	20	22	17
BER	13	22	20	31	25	20	14	29	11	20	11	18
BJO1	32	4	13	9	8	13	14	20	12	16	30	18
BLS5	30	27	35	28	57	19	62	40	35	23	28	24
DOMB	16	34	24	34	27	36	19	65	11	46	12	39
FAUS	83	39	47	35	35	34	94	47	47	62	51	51
FOO	5	4	17	19	43	16	24	31	23	18	16	16
HAMF	23	28	10	32	12	42	22	78	8	51	38	47
HOMB	13	17	18	26	19	19	33	29	23	18	17	18
HOPEN	66	14	58	17	53	12	54	20	41	12	86	28
HYA	28	19	30	20	63	19	48	36	37	21	23	17
JMI	30	0	7	0	10	0	27	0	19	0	125	0
JMIC	37	2	8	3	9	1	28	6	21	3	129	0
JNE	24	0	6	0	10	0	25	0	18	0	116	0
JNW	31	1	7	0	10	0	27	1	22	0	126	0
KBS	109	12	87	22	94	14	87	22	93	18	99	29
KMY	20	13	24	14	38	18	48	26	32	15	20	16
KONO	22	21	24	35	34	35	23	58	13	29	17	37
KONS	86	30	32	29	48	23	138	53	60	9	132	33
KTK1	122	41	47	37	50	46	50	82	33	63	65	57
LOF	37	29	17	28	12	35	58	66	47	41	37	40
MOL	13	26	5	18	16	26	9	44	8	29	10	27
MOR8	77	40	19	8	55	40	137	63	80	63	88	47
NSS	14	37	7	33	8	41	24	69	13	59	16	43
ODD1	31	29	41	30	71	21	66	44	25	20	17	16
OSL	4	24	9	31	8	31	7	51	0	21	1	28
SKAR	41	34	50	38	83	35	64	62	42	41	31	36
SNART	20	16	21	28	33	20	42	36	31	22	19	16
STAV	7	9	11	17	13	16	16	21	9	18	4	15
STEI	74	38	30	22	25	44	136	71	69	57	71	50
STOK	69	11	48	8	48	23	141	37	72	16	101	12
SUE	17	12	24	16	56	15	37	30	26	13	18	13
TBLU	3	14	1	7	0	7	0	22	0	21	3	10
TRO	33	37	9	35	5	49	10	65	7	60	19	50
NORSAR	14	59	8	38	23	68	30	95	22	95	14	79
ARCES	151	39	107	32	95	44	86	83	73	64	84	56
SPITS	125	31	104	31	103	31	87	49	82	37	110	47

Table 8. Monthly statistics of events recorded at each station for July-December 2015. Abbreviations are: L = Number of local events recorded at more than one station and D = Number of teleseismic events recorded at the station.

	JULY		AUGUST		SEPT		OCT		NOV		DEC	
STATION	**L**	**D**	**L**	**D**	**L**	**D**	**L**	**D**	**L**	**D**	**L**	**D**
ASK	38	34	33	24	47	21	14	10	31	35	23	20
BER	28	33	17	26	20	23	13	24	12	34	14	21
BJO1	41	46	37	25	20	27	12	20	24	27	14	11
BLS5	37	33	41	25	43	31	22	26	24	19	18	16
DOMB	19	69	19	43	15	12	26	55	21	75	17	38
FAUS	64	91	88	63	89	83	86	60	109	80	90	43
FOO	29	27	30	22	26	25	25	18	22	24	23	14
HAMF	55	80	36	60	18	64	33	46	41	68	22	31
HOMB	23	23	19	19	18	27	18	25	32	41	14	17
HOPEN	112	39	78	19	37	15	43	13	46	25	38	8
HYA	36	29	37	26	47	22	39	21	42	30	32	13
JMI	113	0	46	0	25	0	21	1	16	0	15	0
JMIC	117	6	54	2	26	0	29	6	18	7	17	1
JNE	118	0	47	0	21	0	24	0	14	0	14	0
JNW	118	0	53	0	26	0	25	0	17	0	15	0
KBS	155	41	98	26	70	18	73	17	71	28	56	13
KMY	33	23	33	16	36	16	5	2	24	20	5	6
KONO	29	59	21	36	17	30	35	41	65	67	39	31
KONS	118	63	118	41	93	58	85	43	105	66	92	32
KTK1	96	90	127	66	106	73	111	61	75	68	78	45
LOF	40	76	36	49	32	60	38	47	20	66	21	21
MOL	15	54	17	39	12	40	13	38	10	46	11	21
MOR8	84	82	92	56	84	76	68	55	91	67	71	30
NSS	18	82	21	56	16	62	11	49	8	78	17	37
ODD1	26	31	16	12	22	17	22	32	26	40	14	17
OSL	8	50	6	33	9	23	17	38	32	51	22	20
SKAR	48	71	53	49	70	43	76	50	106	62	71	34
SNART	28	32	22	19	23	19	11	18	31	29	15	11
STAV	20	24	9	8	11	13	3	16	6	23	7	11
STEI	55	88	66	52	63	75	64	53	46	72	43	31
STOK	92	28	85	16	58	17	49	11	68	38	72	14
SUE	28	23	34	21	41	21	32	18	26	22	23	12
TBLU	0	0	0	7	1	7	5	27	1	25	2	18
TRO	26	90	20	63	12	67	20	57	16	78	17	37
NORSAR	12	107	18	98	9	96	18	70	13	61	17	63
ARCES	120	89	136	60	83	69	111	59	130	74	97	44
SPITS	174	69	106	49	78	50	88	52	81	68	66	39

4.3 The seismicity of Norway and adjacent areas

The main area of interest is defined as 54-82N and 15W-35E, Figure 7. We also show the seismicity for the Arctic region including the Barents Sea defined by coordinates 65-85°N and 20°W-50°E. A total of 4153 of the recorded events are located inside the NNSN prime area. During analysis and using the explosion filter (Ottemöller, 1995), 40% of these events were identified as confirmed or probable explosions or induced events. After including stations located on the eastcoast of Greenland, operated by GEUS, the number of located events has increased in the Artic area. Figure 7 shows all local/regional events in the prime area, analysed and located during 2015. Among these, 451 are located in the vicinity of Jan Mayen.

Figure 8 shows the location of every earthquake (known and probable explosions removed) located within the prime area with one of the calculated magnitudes above 3. Table 9 lists the same earthquakes with all earthquakes located close to the Mid-Atlantic ridge removed.

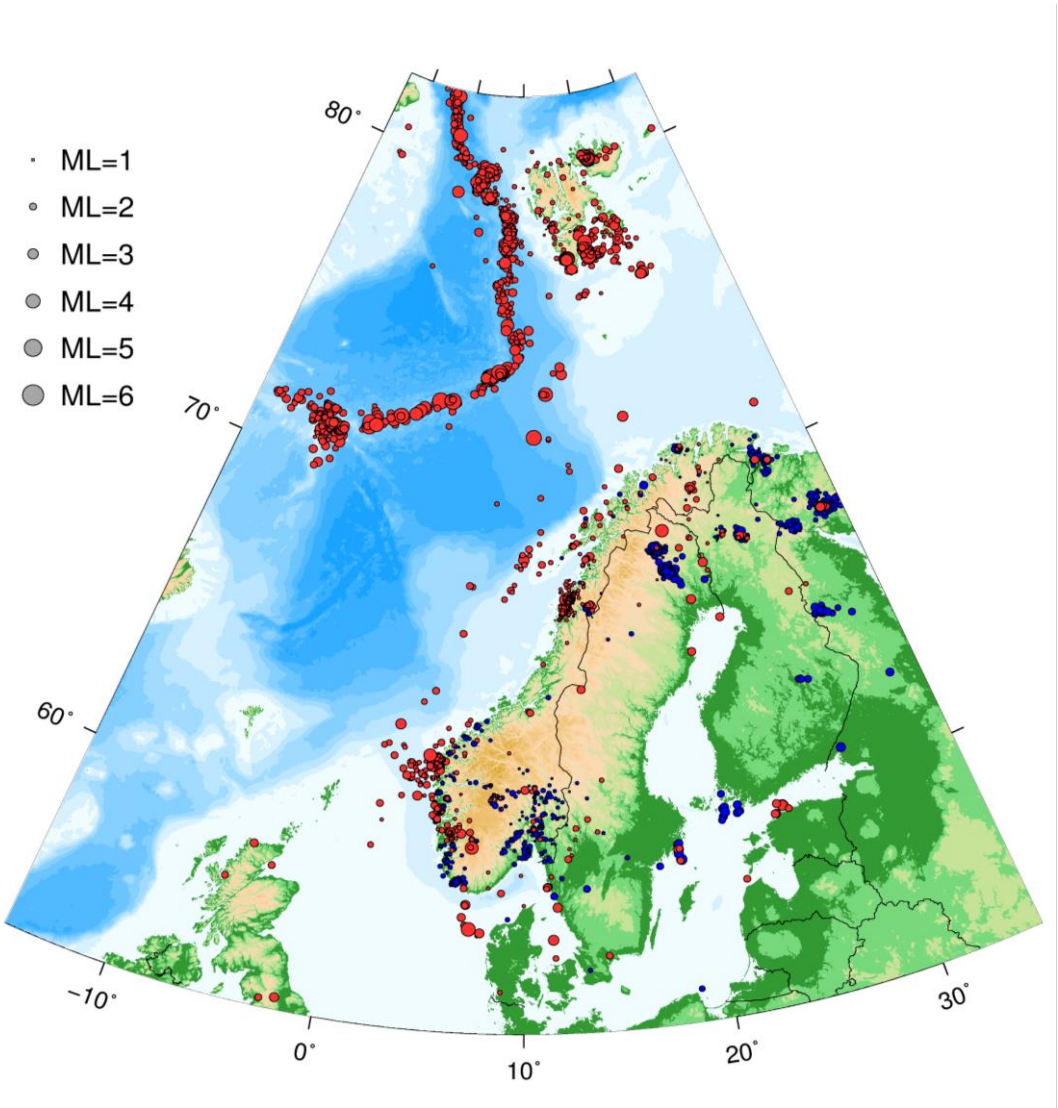

Figure 7. Epicentre distribution of events analysed and located in 2015. Earthquakes are plotted in red and probable and known explosions in blue. For station locations, see Figure 1.

It should be emphasized that the magnitude calculation for the earthquakes located on the oceanic ridge in the Norwegian Sea uses the same formula as for mainland Norway. As the scale is not appropriate for this region, the magnitudes for these earthquakes are underestimated. Most of the recorded earthquakes in this area have magnitudes above 3.0 if they are recorded on Norwegian mainland stations. A new magnitude scale for the artic area is expected to be available during 2016.

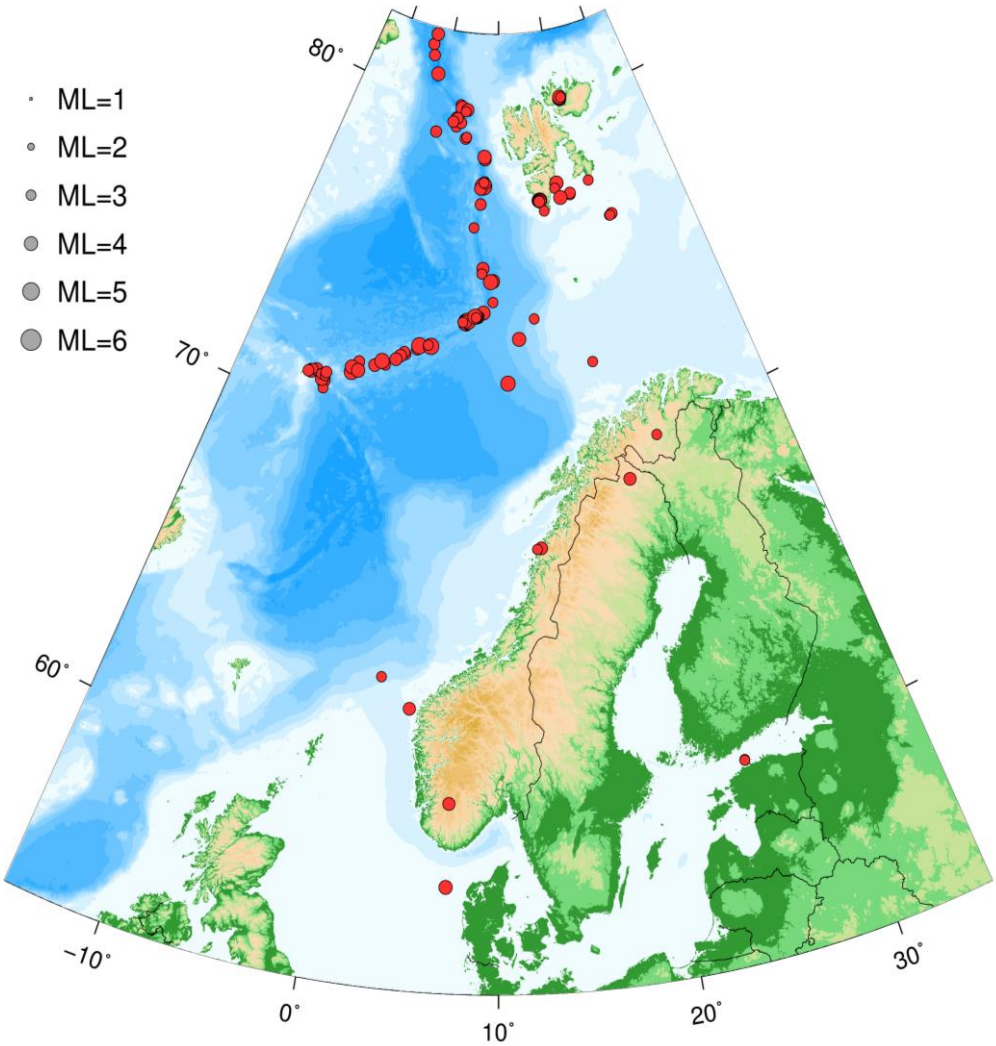

Figure 8. Epicentre distribution of located events with one of the calculated magnitudes above or equal to 3.0. For station location, see Figure 1.

The largest local or regional earthquake in 2015, recorded on Norwegian stations and within the prime area, occurred on December 21st at 10:31(UTC) offshore the Danish west coast. The earthquake had a magnitude of $M_{L(BER)}$=3.2, M_L=3.3 reported from GEUS, Denmark and M_L=4.0 reported from BGS.

Along the mid-Atlantic ridge a large number of earthquakes occur with magnitude above 3 which is approximately the detection level along the Mohns ridge. Of the 32 located earthquakes with magnitude above 4, 23 were located along the ridge mostly along the Mohns ridge. The magnitudes calculated for earthquakes in the Norwegian-Greenland Sea are expected to be underestimated.

Table 9. Earthquakes located in the vicinity of mainland Norway and in the Svalbard area (grey background) with any reported magnitude above or equal to 3.0 for the time period January through December 2015. In cases where all BER magnitudes are below 3 but the event still is included in the list, NORSAR (NAO), GEUS- Geological Survey of Denmark and Greenland (DNK), University of Uppsala (UPP), University of Helsinki (HEL) or the British Geological Survey (BGS) has reported a magnitude of 3.0 or larger. Abbreviations are: HR = hour (UTC), MM = minutes, Sec = seconds, L = distance identification (L=local, R=regional, D=teleseismic), Latitud = latitude, Longitud = longitude, Depth = focal depth (km), F = fixed depth, AGA = agency (BER=Bergen), NST = number of stations, RMS = root mean square of the travel-time residuals, Ml = local magnitude and Mw = moment magnitude.

Year	Date	HRMM	Sec	L	Latitud	Longitud	Depth	F	AGA	NST	RMS	Ml	Mw	ML (NAO)	ML
2015	120	0131	33.0	L	76.972	18.729	2.8		BER	9	0.6	2.6		3.0	
2015	128	0318	16.0	L	71.967	19.500	15.0	F	BER	19	0.7	2.1		3.1	
2015	407	1138	37.4	L	77.008	20.023	15.0		BER	14	0.6	2.7		3.3	
2015	424	0940	38.5	L	66.661	13.290	2.0	F	BER	48	0.8	3.2			3.3(UPP)
2015	429	2246	21.1	L	59.270	7.065	15.0		BER	52	0.5	3.5		3.6	3.7(DNK)
2015	5 6	0336	26.4	L	77.029	20.036	15.0		BER	7	0.6	2.4		3.5	
2015	511	0613	44.7	L	76.966	18.807	20.8		BER	13	0.7	3.0		3.2	
2015	618	0918	4.4	L	68.400	20.918	14.1		BER	40	0.7	3.2		3.8	
2015	618	2121	13.8	L	71.553	10.968	23.6		BER	57	0.7	3.1		4.3	
2015	702	1703	34.5	L	57.624	6.914	12.7		BER	20	0.7	2.6		2.4	3.1(DNK)
2015	7 4	0742	27.1	L	76.954	15.764	1.6		BER	26	0.7	3.7		4.5	
2015	7 4	0744	48.0	L	76.945	15.613	0.7		BER	8	0.3	3.4		4.0	
2015	7 7	2017	35.1	L	80.027	20.905	15.0		BER	6	0.7	2.6		3.0	
2015	708	1432	13.9	L	57.288	6.757	15.0	F	BER	32	0.7	2.4		2.4	3.3(DNK)
2015	710	2240	1.0	L	62.769	2.222	15.7		BER	54	0.6	2.6		3.0	3.2(BGS)
2015	713	0352	58.9	L	79.889	21.028	15.0		BER	16	0.6	3.0		3.7	
2015	717	1236	26.6	L	79.935	21.232	15.0		BER	11	0.7	2.8		3.5	
2015	717	2239	13.9	L	80.005	21.218	15.0		BER	22	0.8	3.4		4.2	
2015	729	1916	2.8	L	57.589	11.801	14.0		BER	40	0.6	2.6	2.7	2.9	3.0(DNK)
2015	8 7	1616	12.0	L	76.953	15.702	4.2		BER	9	0.5	3.1		3.6	
2015	8 8	2354	56.0	L	76.929	15.761	6.0		BER	23	0.6	3.4		4.0	
2015	8 9	0016	57.1	L	76.926	15.683	5.8		BER	15	0.5	3.1		3.4	
2015	8 9	0218	59.7	L	76.927	15.743	4.9		BER	14	0.7	2.7		3.1	
2015	809	2257	8.9	L	66.627	13.004	15.0		BER	11	0.6	2.8	3.0	3.1	3.0(HEL)
2015	1014	2005	31.6	L	79.934	21.094	19.0		BER	21	0.6	3.4		4.1	
2015	1024	0303	4.0	L	76.648	16.358	3.4		BER	10	0.5	2.7		3.0	
2015	11 8	1203	41.8	L	77.303	22.975	22.7		BER	16	0.3	3.0		3.2	
2015	11 9	0355	40.2	L	79.925	21.299	15.0		BER	10	0.9	3.0		3.4	
2015	1119	1418	37.1	L	56.885	8.044	10.0	F	BER	52	0.6	2.8	2.6	2.7	3.7(BGS)
2015	1120	2354	2.5	L	77.024	18.604	21.8		BER	11	0.5	2.8		3.0	
2015	1122	0005	30.2	L	77.398	18.425	22.7		BER	22	0.4	3.7	3.5	4.0	
2015	1126	1529	8.2	L	77.254	18.026	15.0		BER	9	0.7	2.5		3.0	
2015	12 2	0937	54.9	L	76.960	18.662	15.0		BER	19	0.7	3.2	3.6	4.0	
2015	1211	0720	45.7	L	61.917	4.325	17.0		BER	60	0.5	3.4	3.7	3.5	3.8(BGS)
2015	1219	0829	6.3	L	76.151	25.037	20.9		BER	16	0.6	2.9	3.3	3.4	
2015	1220	0747	38.3	L	76.130	24.711	21.1		BER	15	0.6	2.5	3.0	3.3	
2015	1220	2240	42.4	L	76.121	24.769	19.8		BER	18	0.6	3.0	3.1	3.6	
2015	1221	1031	6.6	L	56.954	7.157	16.1		BER	45	0.6	3.2		3.2	4.0(BGS)
2015	1231	1513	42.5	L	76.911	15.664	4.0		BER	14	0.4	2.9	3.4	3.3	

The most significant earthquakes during 2015 and located in the vicinity of the Norwegian mainland were:

- December 11th 2015, 07:20(UTC) located offshore Stadt with a magnitude of M_W=3.7. This earthquake was reported felt in Sogn and Fjordane (Figure 18).
- Offshore Denmark an earthquake occurred December 21st at 10:31(UTC), magnitude 3,2L_{BER} , 3.3L_{DNK} and 4.0L_{BGS} located to 56.95N 7.16E.

- In the Storfjorden, Svalbard area there are located 19 earthquakes with at least one reported magnitude above 3.0. The largest occurred July 4th at 07:42 located to 76.95N 15.76E with magnitudes ML_{BER} =3.7, ML_{NAO} =4.5

4.3.1 Seismicity in Nordland

Figure 9 shows the seismicity in Nordland since 2000. The area includes the locations of earthquake swarm activity such as Meløy, Steigen and Stokkvågen. The latter two areas are clearly visible on the map. Steigen was active between 2007 and 2008, but has been relatively quiet until 2015 when 44 earthquakes are located to the area.

The activity in the Stokkvågen area has been nearly continuous, and specific clusters in time and space have occurred. Figure 10 shows the seismicity in the area during 2015. As can be seen from the figure the seismic activity is located to the already known active areas. The increased station-density in the area lowered the detection threshold and more events with low magnitude are located.

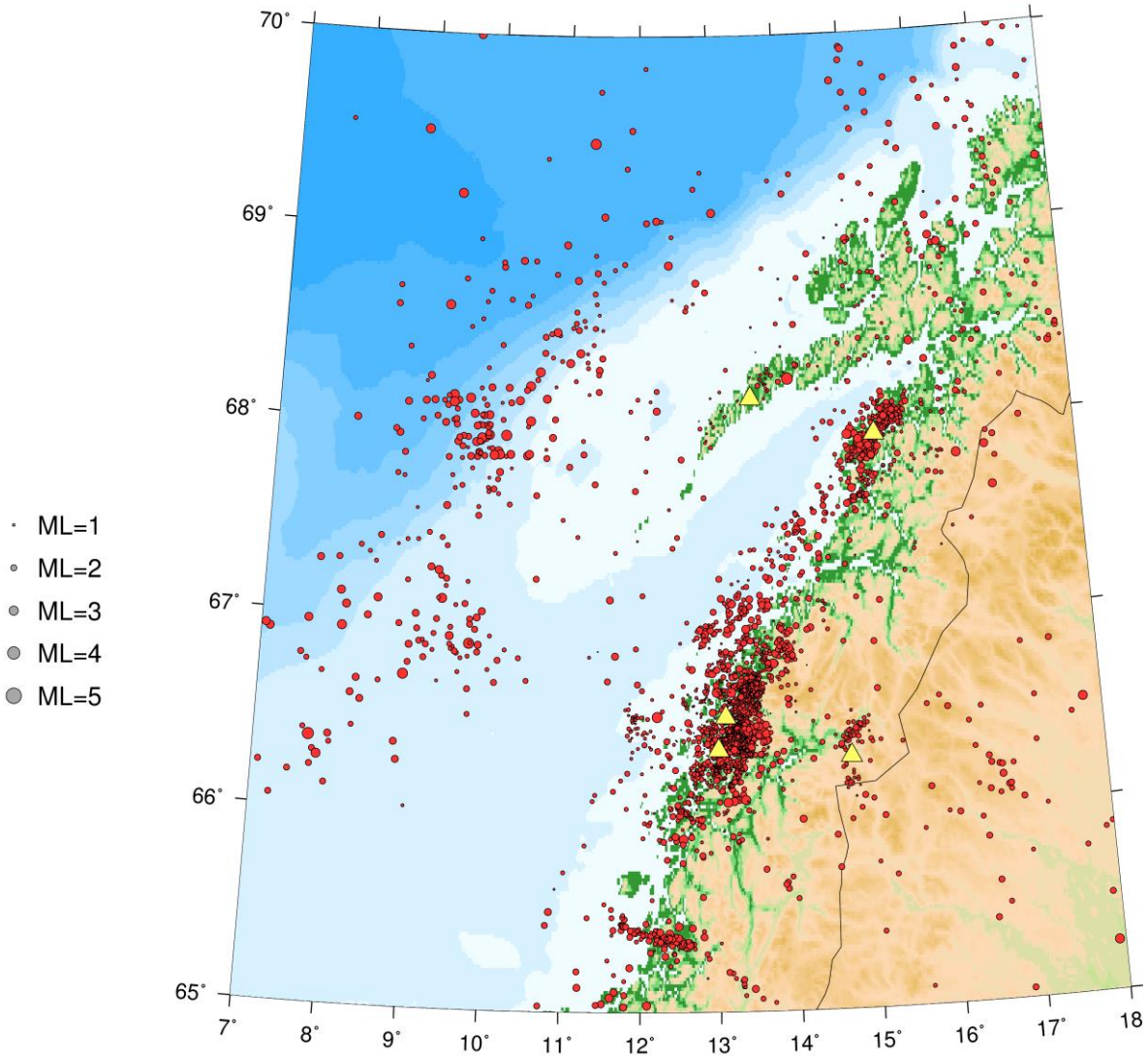

Figure 9. Seismicity in the Nordland area. Red circles show seismicity for 2000-2015, and yellow triangle is NNSN seismic stations. Known and probably explosions are excluded.

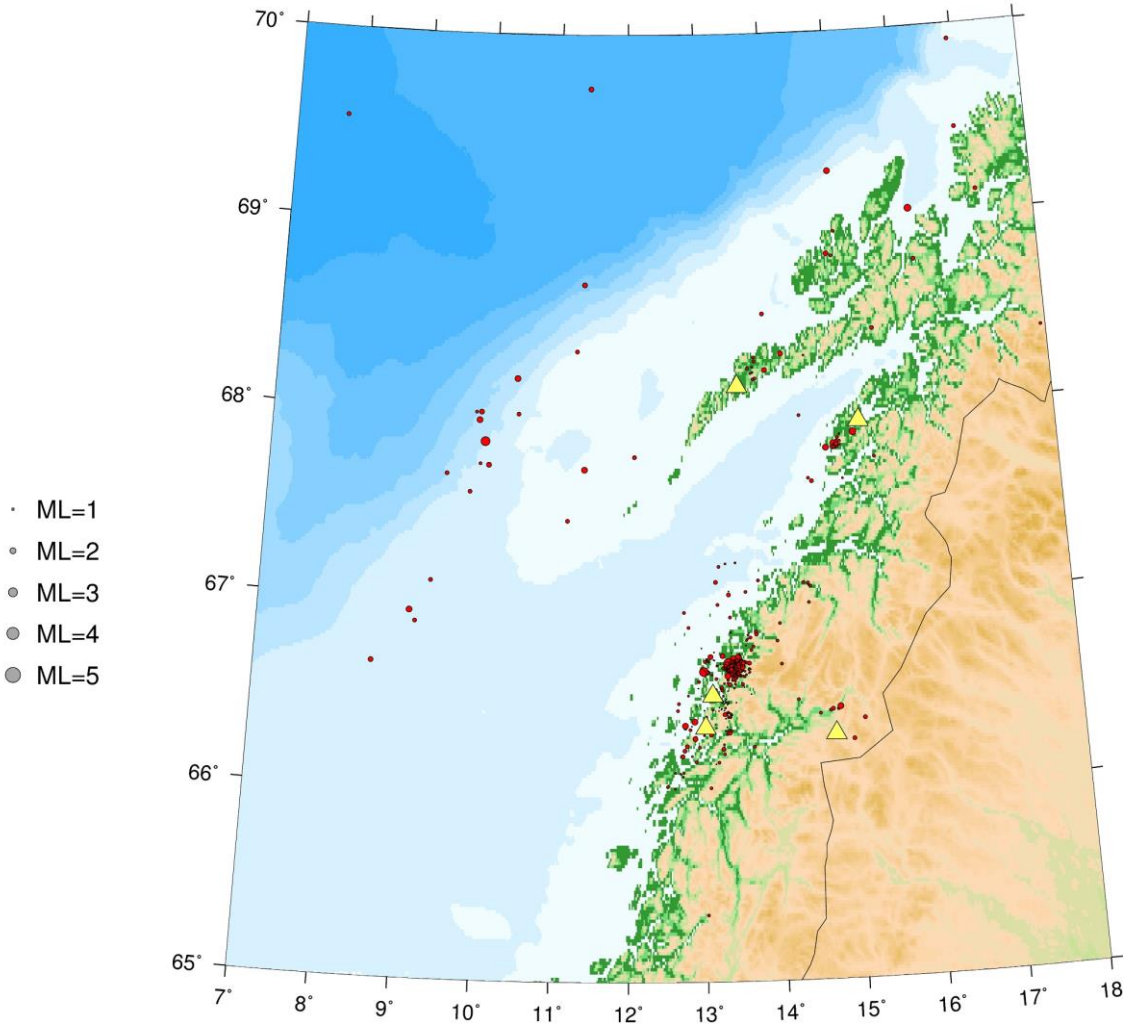

Figure 10 Seismicity in the Nordland area. Red circles show seismicity for 2015, and yellow triangle is NNSN seismic stations. Known and probably explosions are excluded.

In the Jektvik (66.6N,13.5E) and also in the Steigen (68N,15E) area there has been an increased seismic activity during 2015 compared to 2014. In the Jektvik area the earthquakes are located onshore to the area southwest of the Svartisen glacier. During 2015, 476 earthquakes are located to this area compared to 71 in 2014. The earthquake swarm started in April 2015 as can be seen in Figure 11. Early in the swarm sequence three larger earthquakes occurred, see Table 10.

Table 10 The largest (M>3.0) recorded earthquakes located in the swarm area. Two are felt locally.

Year	Date	HRMM	Sec	L	Latitud	Longitud	Depth	AGA	NST	RMS	Ml(BER)	ML(NAO)	FELT
2015	411	0313	30.7	L	66.658	13.370	8.0	BER	42	0.8	2.6	3.1	No
2015	416	0512	31.5	L	66.638	13.438	8.0	BER	23	0.6	2.4	3.0	Yes
2015	424	0940	38.5	L	66.660	13.300	2.0	BER	48	0.8	3.2	3.7	Yes

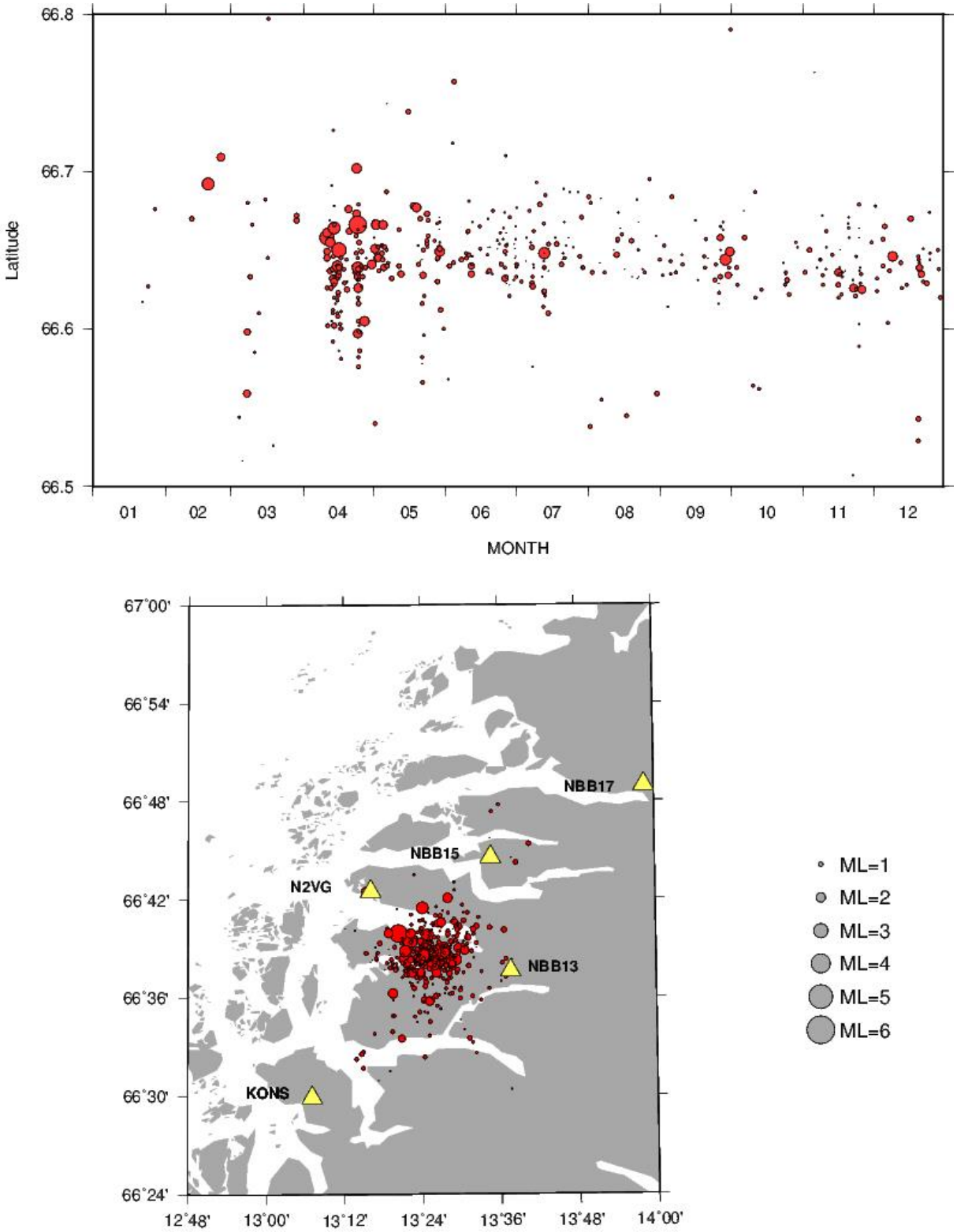

Figure 11 Time distribution (upper) and location (lower) of the earthquake swarm located southwest of the Svartisen glacier. Note! The events shown are limited by 66.5- 66.9N and 13.2-13.7E, a smaller area than show on the map. The location of the permanent NNSN station (KONS) and the NEONOR2 stations (N2VG, NBB13, NBB 15, NBB17) are marked on the map.

The yearly distribution of earthquakes located in the area is presented in Figure 12.

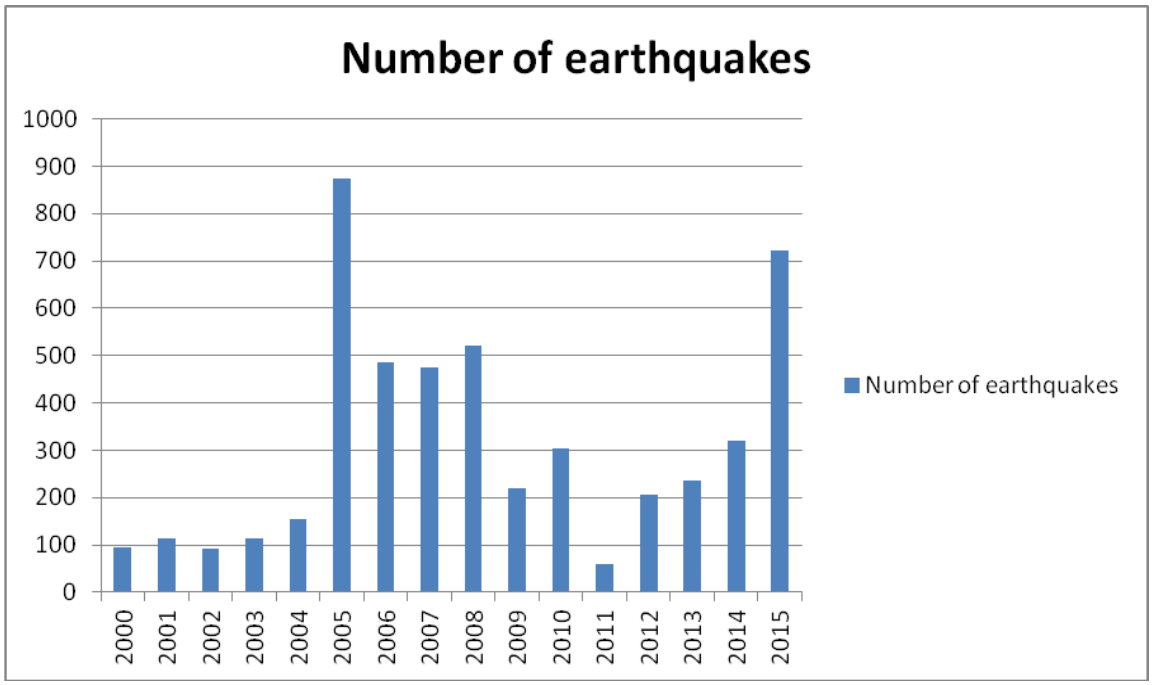

Figure 12 The yearly number of earthquakes in the area shown in Figure 10.

4.3.2 Seismicity in the arctic area

With the mainland stations on the Lofoten, in Tromsø and Hammerfest, the network on Jan Mayen, and stations on Bjørnøya, Hopen and Svalbard, the network detection capability in the arctic area is relatively good. We define the arctic area as the region 65-85°N and 25°W-50°E. Most of the activity falls into three areas: Jan Mayen, the Mid-Atlantic ridge and Storfjorden southeast of Svalbard, as can be seen in Figure 12. Since 2014 data from Danish stations on Greenland (see Figure 2) were included in the daily processing which has increased the location accuracy for earthquakes west of Jan Mayen and northwest of Svalbard. The number of earthquakes recorded on enough stations to be located, have increased.

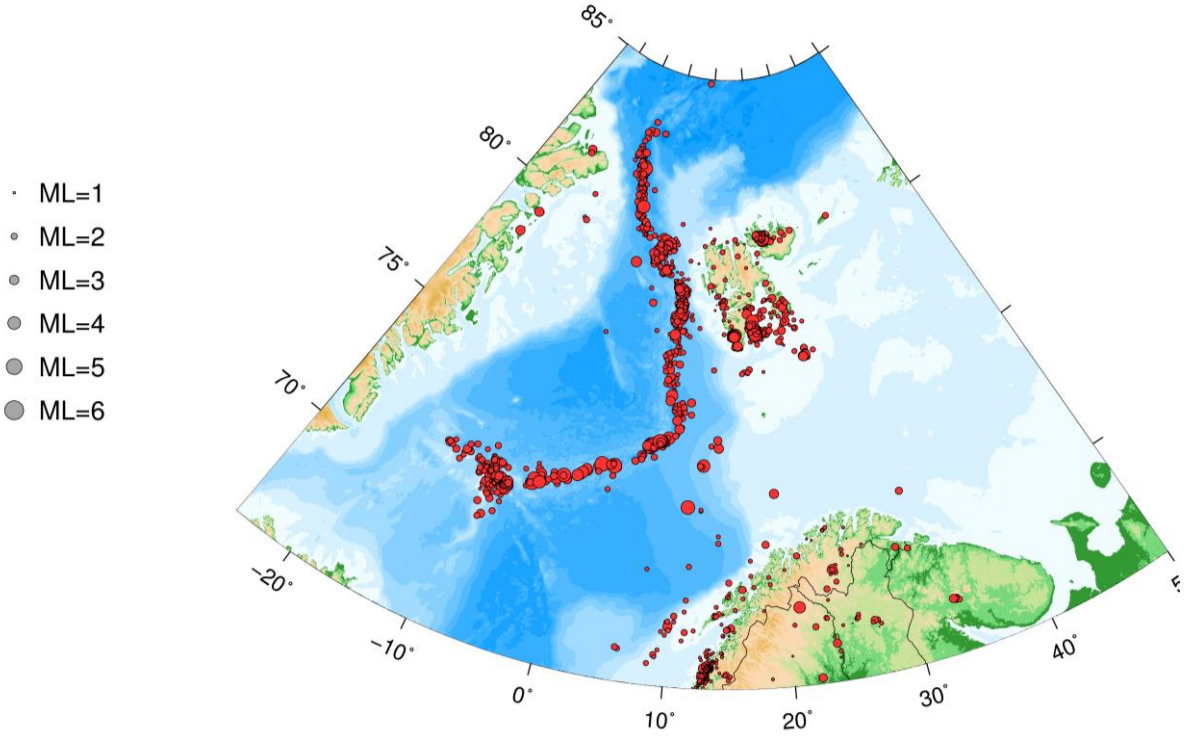

Figure 13. Seismicity in the Norwegian arctic area during 2015. A total of 2252 located earthquakes.

4.3.3 Seismicity in the Jan Mayen area

Jan Mayen is located in an active tectonic area with two major structures, the Mid Atlantic ridge and the Jan Mayen fracture zone, interacting in the vicinity of the island. Due to both tectonic and magmatic activity in the area, the number of recorded earthquakes is higher than in other areas covered by Norwegian seismic stations. During 2015 a total of 430 earthquakes were located as seen in Figure 14 and of these, 12 had a magnitude equal or above 3.0.

The largest earthquake in the Jan Mayen region in 2015 occurred on 30th June at 07:40 (UTC) and the magnitude is estimated to 3.7. The earthquake is located slightly west of the island in the Jan Mayen fracture zone and was felt by the personnel at Jan Mayen.

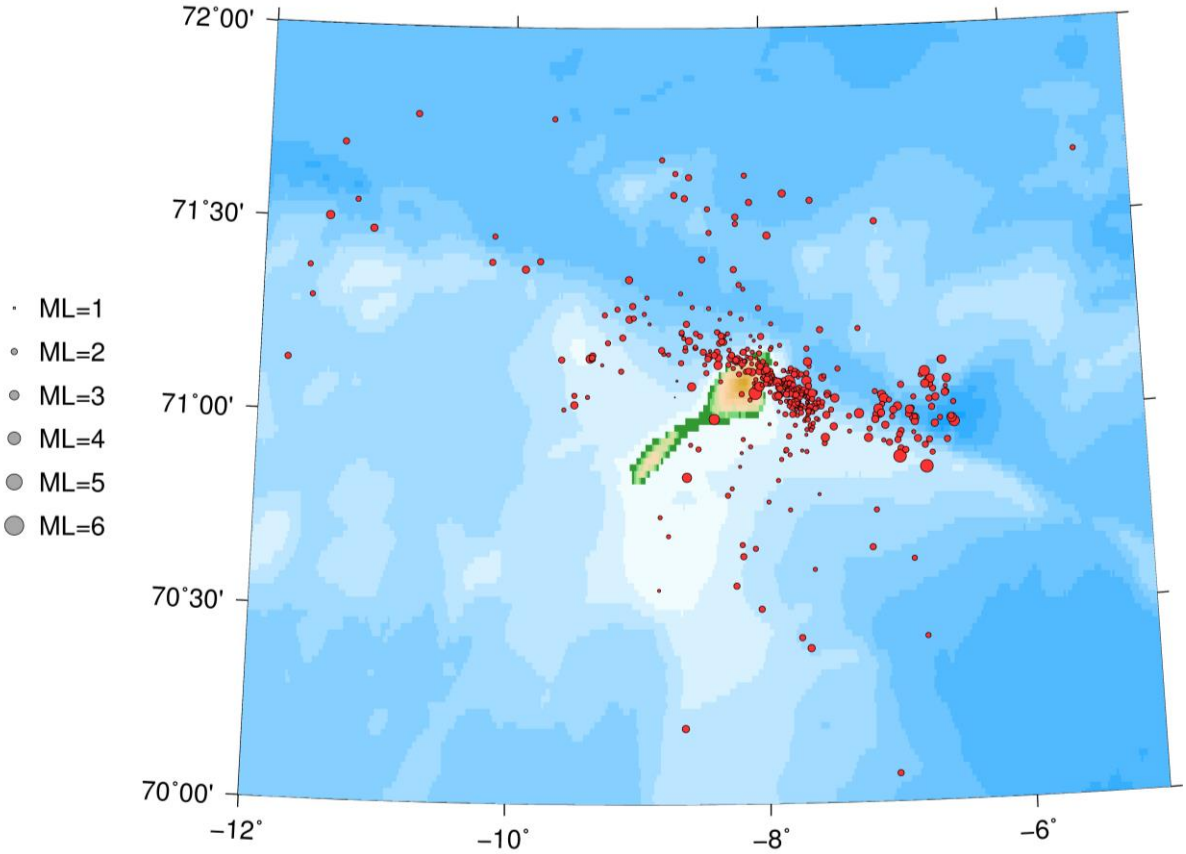

Figure 14. Earthquakes located in the vicinity of Jan Mayen during 2015.

The number of recorded earthquakes in the Jan Mayen area has varied over the last years (Figure 15). The number of relatively strong earthquakes (M≥3) shows smaller time variation than for the smaller earthquakes. The increases in 2004 and 2005 were due to the M=6.0 earthquake in 2004 and its aftershocks (Sørensen et al., 2007). The same is true for 2011, where the M=6.0 earthquake on 29 January was followed by a sequence of aftershocks. The 30 August 2012 earthquake with its fore and aftershocks clearly increases the number of recorded events in 2012 compared with previous years, making it the largest number of recorded events yearly for more than 10 years. For the following years after 2012, the number of located smaller earthquakes has increased slightly, while the number of larger (M≥3.0) earthquakes is relative stable.

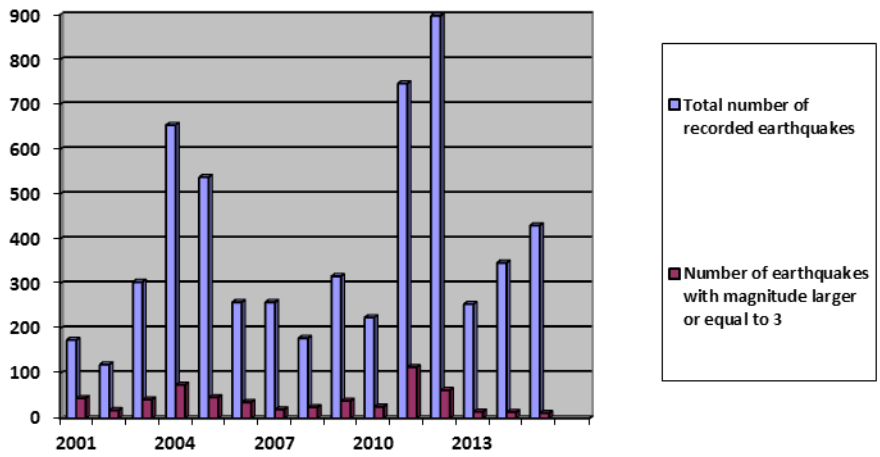

Figure 15. Yearly distribution of earthquakes located in the Jan Mayen area since 2001. The area is as shown in Figure 14.

4.3.4 Seismicity in Storfjorden, Svalbard

The Storfjorden area southeast of Svalbard, defined by latitude 76.5-78N and longitude 16-22E, has been seismically active since the M_w=6.0 earthquake on 21 February 2008. A preliminary study was presented by Piril et al. (2008). One of the main objectives from this study was to resolve the source mechanism, which was found to be oblique-normal. This result was found from the inversion of both regional and teleseismic data. The earthquake had a high number of aftershocks.

A total of more than 35 earthquakes with magnitude larger than M=4 have occurred in the area since 2008. From the monthly number of all detected earthquakes it seems that the activity had decreased until the start of 2009 and then remained relatively low until late 2009. In 2010 the number increased again and remained mostly stable in 2011. This is mostly explained by an increase in the number of smaller earthquakes as seen by the almost constant levels of earthquakes with M>2.5 since 2008. The better detection was due to usage of the data from the Hornsund (HSPB) and Barentsburg stations. It appears as if the overall activity is decreasing slightly, although still continuing. The total number of events located in the Storfjorden area in 2015 was around 176, a decrease compared to the previous years.

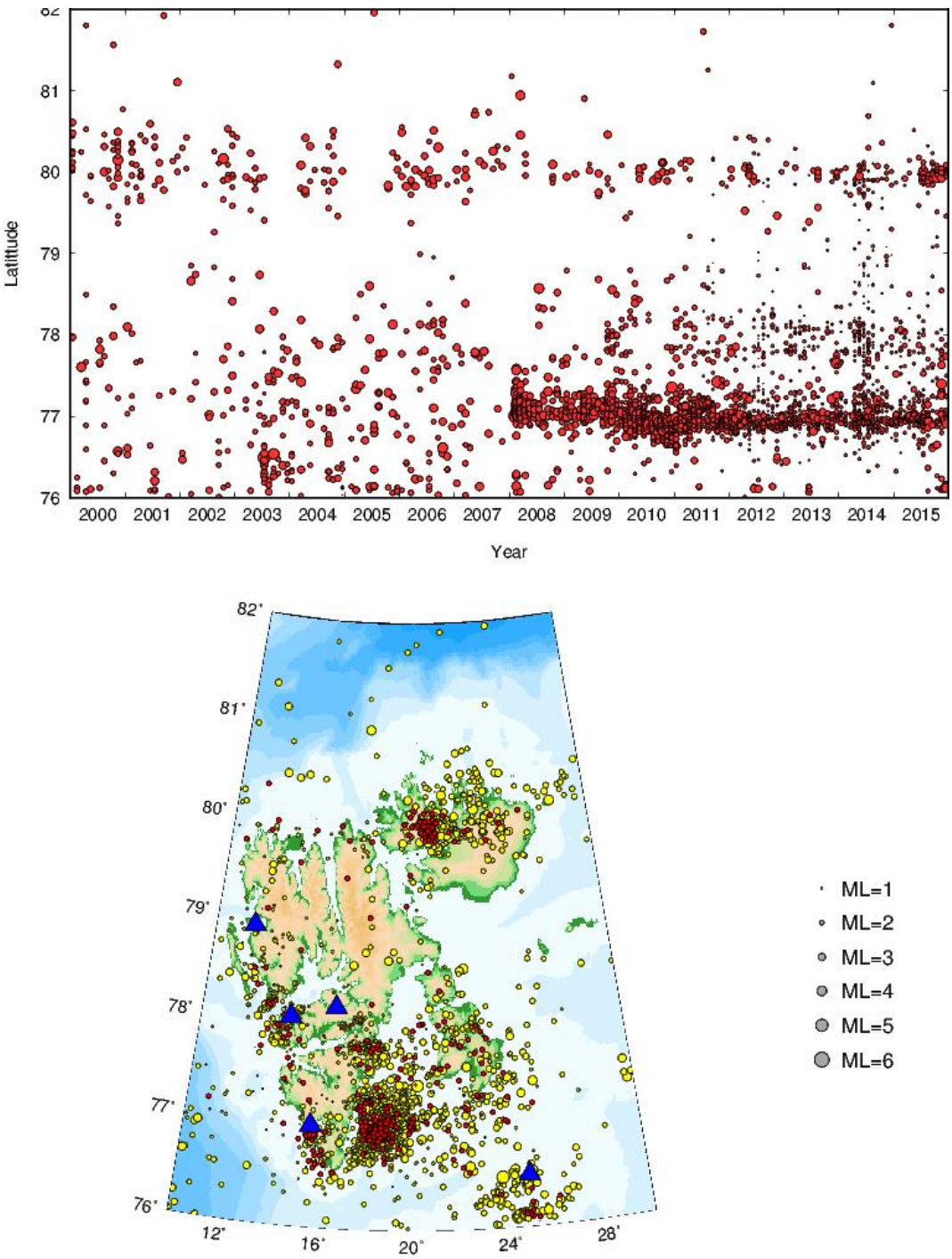

Figure 16 Seismicty in the Svalbard area. Bottom: Earthquakes occurring in 2015 are plotted in red circles. Yellow circles show seismicity for 2000-2014. The blue triangles give the station locations. Top: Seismicity in the same area is plotted as latitude as function of time.

Figure 16 shows both a map with the seismicity since 2000 and the distribution of events over time. The onset of the activity in the Storfjorden area in February 2008 is obvious from the time plot. The seismicity since 2011 is mostly concentrated in the southwestern half of the area that has been active since 2008. The six largest earthquakes, all occurred in the western part of Storfjorden, the largest (M=4.1), can be seen north of the cluster seen on

.

4.3.5 Earthquakes in the southern North Sea

During 2015 three small earthquakes were detected and located in the North Sea as shown in Figure 17 and listed in Table 11.

Table 11. Earthquakes recorded during 2015 and located in the area limited by 54-60N and 1W-5E.

Year	Date	HRMM	Sec	L	Latitud	Longitud	Depth	AGA	NST	RMS	Ml
2015	2 6	1347	10.1	L	59.885	1.975	18.6	BER	10	0.6	1.1
2015	424	1620	32.0	L	59.997	5.000	0.0	BER	8	0.6	0.9
2015	826	1729	37.4	L	59.114	1.549	3.2	BER	16	1.1	1.8

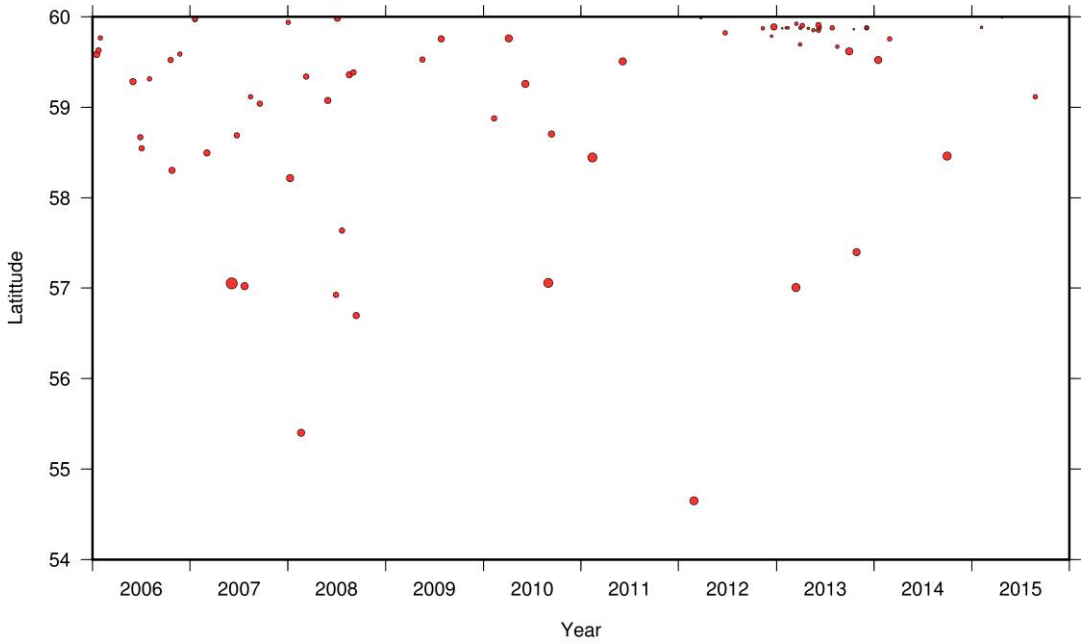

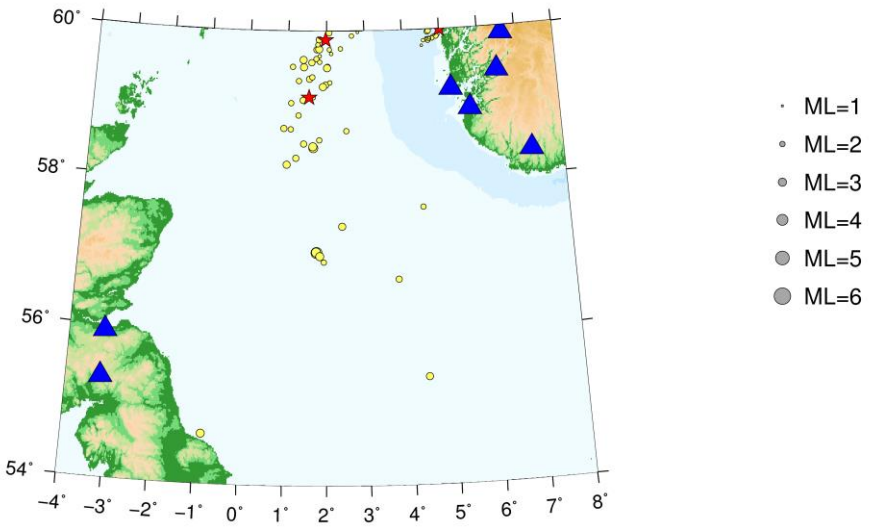

Figure 17. Time distribution (upper) and location (lower) of the earthquake located within 54-60N and 1W-5E in the southern North Sea (Note that the map is larger than the area used for selection of earthquakes). Earthquakes recorded during 2015 are marked in red stars. Seismic stations are marked with blue triangles.

4.3.6 Felt earthquakes

In total, 21 earthquakes were reported felt and located within the target area during 2015 (see Table 12 and Figure 18). Not all earthquakes were felt in Norway. For the Jan Mayen Island and the area southwest of the Svartisen glacier, the number of felt earthquakes is expected to be larger than reported.

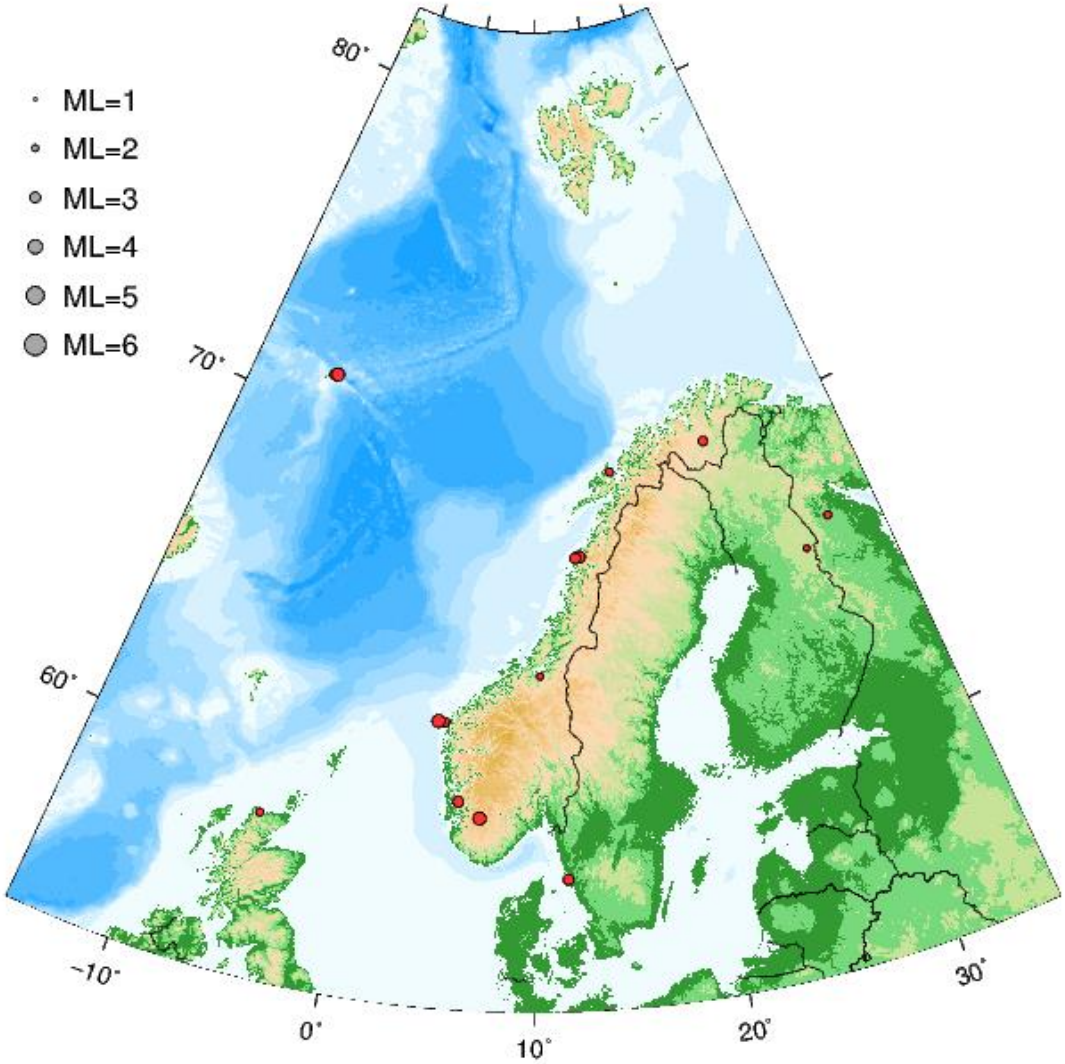

Figure 18. Location of the 20 earthquakes reported felt during 2015. 17 of the earthquakes are felt in Norway including Jan Mayen.

Large felt earthquakes are mostly reported to UiB shortly after the origin time, and location information and questionnaires are available for the public on the site www.skjelv.no. Smaller felt earthquakes may be reported by the public to local newspapers or other institutions and then reported to UiB. Depending on the time-delay for these reports to be available at UiB, the information on web might be accordingly delayed. For any felt earthquake the public has to be made aware of the questionarie, which is done by informing on web and when UiB is contacted by media, private persons or other institutions.

Earthquakes large enough to be felt and occurring in heavily populated areas increases the number of people using the web reporting the intensities. For the earthquake felt in Trondheim October 12th, a small M_L=2.1 earthquake, 1300 people filled in a questionarie and mailed it to Bergen. To be able to process such loads of data, new automatic routines for handling felt earthquakes are under development.

Table 12. Earthquakes reported felt in the BER database in 2015. Abbreviations are: M_L = local magnitude and M_w = moment magnitude, W: questionnaires received on web (Y/N). Earthquakes felt outside Norway are marked in colour.

Nr	Date	Time (UTC)	Max. Intensity (MMI)	Magnitude (BER)	Instrumental epicentre location	W
1	09.01.15	01:03		M_L=2.3, M_L=2.4(BGS)	58.51N / 4.69W	
2	01.02.15	20:24		M_L=2.6, M_L=2.6(NAO)	61.88N / 4.71E	N
3	19.02.15	06:00		M_L=2.5	66.69N / 13.40E	N
4	02.04.15	22:37		M_L=1.8, M_L=1.9(HEL)	65.63N / 29.28E	
5	11.04.15	03:13		M_L=2.6, M_L=2.8(UPP)	66.66N / 13.34E	N
6	12.04.15	11:11		M_L=1.7, M_L=2.3(HEL)	66.66N / 13.34E	N
7	14.04.15	06:07		M_L=2.1, M_L=2.6(HEL)	66.67N / 13.29E	N
8	15.04.15	16:08		M_L=1.9, M_L=2.2(NAO)	66.63N / 13.40E	N
9	16.04.15	05:12		M_L=2.4, M_L=3.0(NAO)	66.64N / 13.28E	N
10	24.04.15	09:40		M_L=3.2, M_L=3.7(NAO)	66.66N / 13.29E	Y
11	29.04.15	22:46		M_L=3.5,M_L=3.6(NAO), M_L=3.7(DNK), M_L=2.5(UPP)	59.27N / 7.06E	Y
12	30.06.15	06:32		M_L=3.1, M_L=4.2(NAO)	71.06N / 8.07W	Y
13	30.06.15	07:40		M_L=3.7	71.09N / 7.80W	N
14	23.07.15	10:31		M_L=2.7,M_W=2.8, M_L=2.9(NAO)	59.69N / 5.86E	Y
15	29.07.15	19:46		M_L=2.6,M_W=2.7, M_L=2.9(NAO)	57.59N / 11.80E	
16	01.08.15	11:42		M_L=2.7,M_W=2.8, M_L=3.2(NAO)	69.44N / 24.10E	N
17	09.08.15	22:57		M_L=2.8,M_W=3.0, M_L=3.1(NAO)	66.63N / 13.00E	Y
18	11.09.15	19:23		M_L=2.6(NAO), M_L=2.5(HEL)	66.32N / 31.46E	
19	12.10.15	20:24		M_L=2.1, M_L=2.0(NAO)	63.30N / 10.43E	Y
20	17.11.15	16:14		M_L=2.0,M_W=2.3, M_L=2.4(NAO)	69.03N / 16.15 E	Y
21	11.12.15	07:20		M_L=3.4,M_W=3.7, M_L=3.8(BGS)	61.91N / 4.34E	Y

The largest felt earthquake during 2015 was the earthquake occurring 29th April at 22:46 (UTC time). The earthquake was reported felt in most part of southwest Norway. Questionnaires were published on web, and UiB received 144 answers. Analysts have not manually checked the intensities so anomalies might occur.

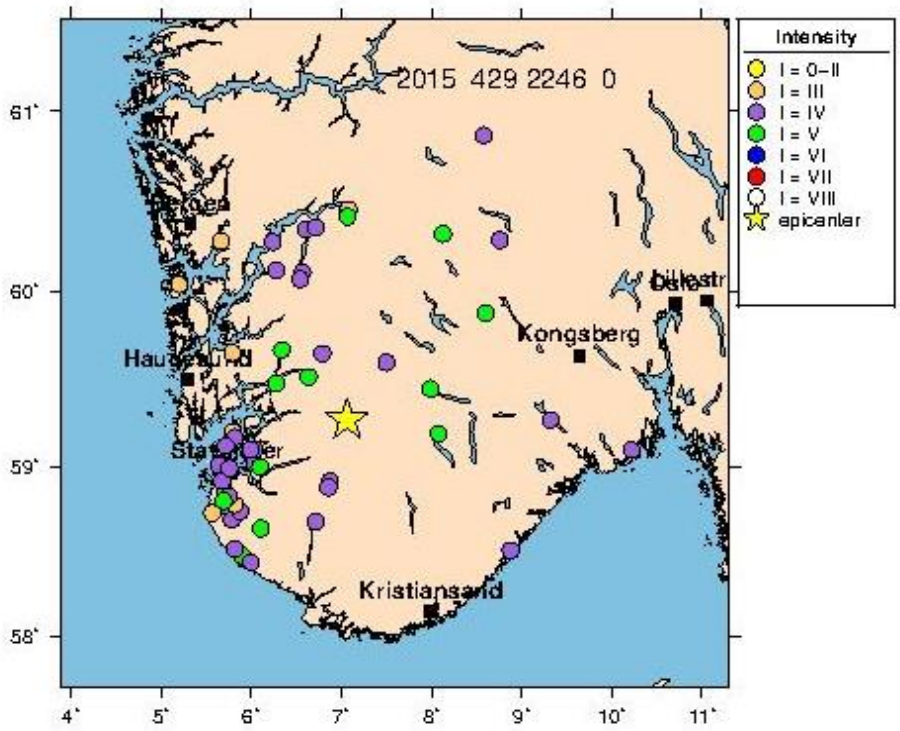

Figure 19. Reported intensities for the earthquake 29th April at 22:46. The yellow star marks the instrumental location.

5 Scientific studies

This section will present an overview of research work that is carried out under the NNSN project. The main objective of this work is to improve the understanding of earthquakes and the seismological models in the region, mostly by using data recorded by the NNSN. Results will be used to improve the NNSN monitoring service.

5.1 P-wave polarization at NNSN for the investigation of local anisotropy and lateral heterogeneity

by Luigia Cristiano, Kiel University

Three-component data from the Norwegian National Seismic Network are suitable to apply polarization analysis (*e.g.*, Jurkevics, 1988; Schulte-Pelkum *et al.*, 2001) to estimate anomalies of wave polarization induced by local wave speed anisotropy and lateral heterogeneities. Long recording time and high quality data guarantee in fact a good azimuthal distribution of events with high signal-to-noise ratio (SNR). Polarization analysis is mainly used as a single method to investigate the characteristics of particle motions**.** We expect that polarization and propagation direction of P waves are both affected by seismic anisotropy as well as by lateral heterogeneities but with different sensitivities.

Polarization parameters are finite frequency observables mostly related to structures up to about one wavelength from the receiver area. The propagation vector direction is also sensitive to distant heterogeneities and distant anisotropy. By polarization analysis we can estimate the deviation of the P-wave polarization vector and its dependence on event backazimuth, epicentral distance and frequency.

The analysis has been applied to almost 20 years (short period as well as broadband) of NNSN data to investigate anisotropy of seismic velocities and lateral heterogeneities beneath the stations. Altogether about 1000 first arriving teleseismic P waves were analyzed. All events with high SNR have been selected and a good distribution in backazimuth and distance (Figure 20) could be obtained.

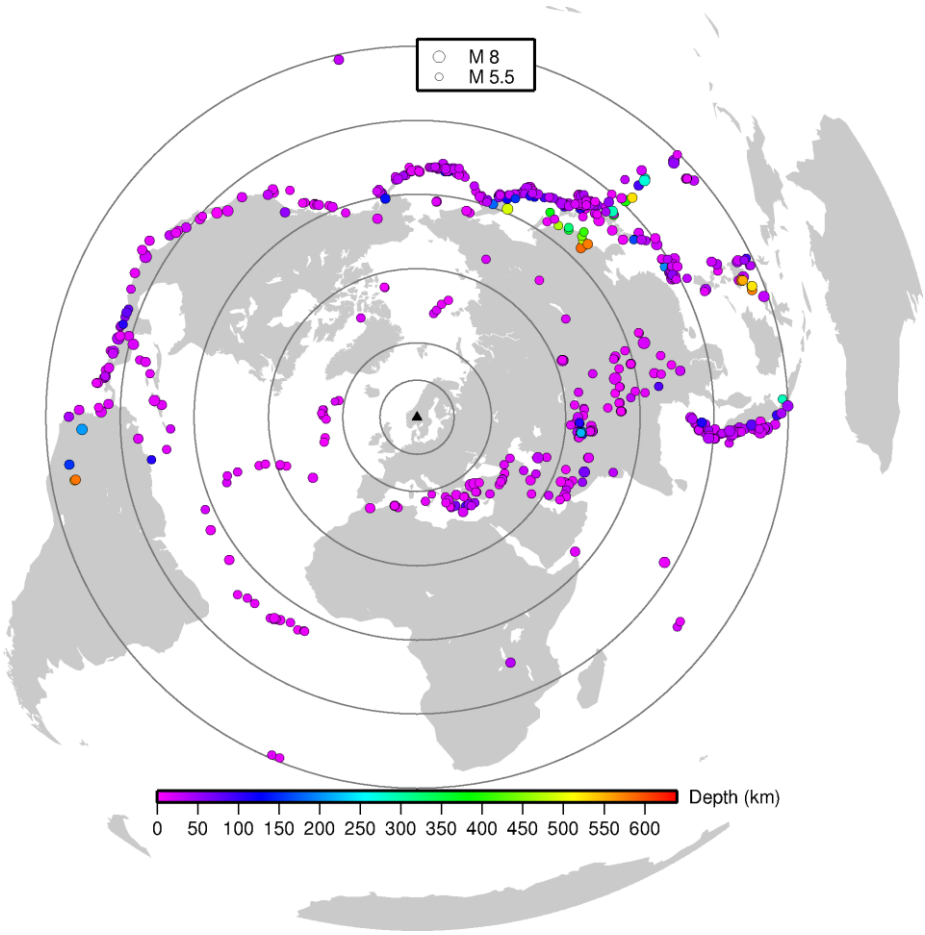

Figure 20. Location of the teleseismic events for which the polarization of the first P-wave arrival has been estimated.

P-wave polarization parameters namely azimuthal deviation and incidence angle have been estimated by solving the eigenvalue problem of the 3-component signal covariance matrix in a moving window following the algorithm proposed by Jurkevics (1988). The parameters have been calculated for each 3C-station of the NNSN in 3 frequency bands (0.02-0.1 Hz, 0.1-0.5 Hz and 0.5-1 Hz). An automated picking algorithm has been used to estimate the polarization parameters of the first P-wave onset including a measure for the quality of the estimate (Cristiano *et al.*, in preparation). Also the azimuthal deviation of the P-wave polarization is mainly dependent on the backazimuth and the frequency. Therefore, we do not separate measurements related to events with different epicentral distances.

It has been observed that the azimuthal deviations are mainly a function of backazimuth and frequency. To investigate the characteristic of this dependence we apply a harmonic analysis (Figure 21). We assume that the azimuthal deviations can be expressed as sum of cosine functions of backazimuth with different periodicities. For each component it is possible to estimate amplitude (A_k) and phase (phi_k). The 360° periodicity in the backazimuth anomalies can be generated by a velocity gradient *e.g.*, caused by a dipping interface (see *e.g.*, Niazi, 1966). From the phase of the 360° term it is possible to determine the strike of the structure showing the velocity gradient and the direction to the low velocities. The 180° periodicity term can be explained in terms of azimuthal anisotropy with a horizontal symmetry axis. From the phase of this harmonic it is possible to estimate the direction of the fast axis of anisotropy.

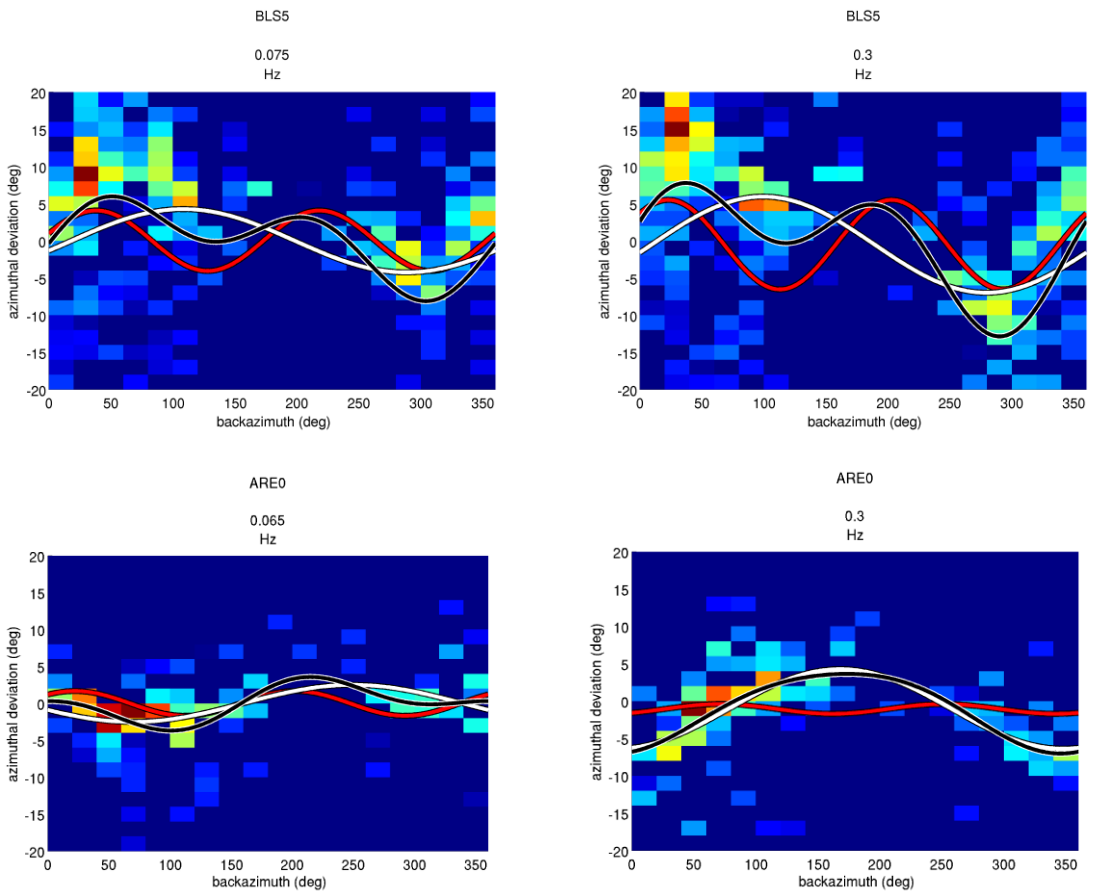

Figure 21. 2D histogram of the azimuthal deviations estimated by polarization analysis at the NNSN sites BLS5 and ARE0 in two frequency bands (0.05 – 0.1Hz, 0.1 – 0.5 Hz). The measurements are distributed in bins on azimuthal deviation and backazimuth ranges. Colors are used to show which bins have the higher number of high quality measurements. Plotted as overlay are the cosine functions with 360 and 180 periodicity from the applied harmonic analysis. The minimum and maximum of the color scale is in dark blue and red respectively.

Harmonic analysis has been applied on the azimuthal deviations estimated by polarization analysis. The dominant periodicities are 360° and 180° for each station of the NNSN but the 180° term is only significant at some sites. We do not observe a marked dependence on the

fast directions of anisotropy on the frequency. This points to the presence of a dominant fast direction in the shallow and deeper crust. At the NORSAR array the directions of fast axis of anisotropy, estimated by polarization analysis are significant only at NC204 and NC303 and only for low frequency observations. The fast directions are 110° with an uncertainty of few degrees and fully consistent with fast directions estimated by Roy & Ritter (2013) applying the SKS/SKKS splitting method. The fast directions of anisotropy retrieved at the stations of NNSN show consistency between neighboring stations (Figure 22).

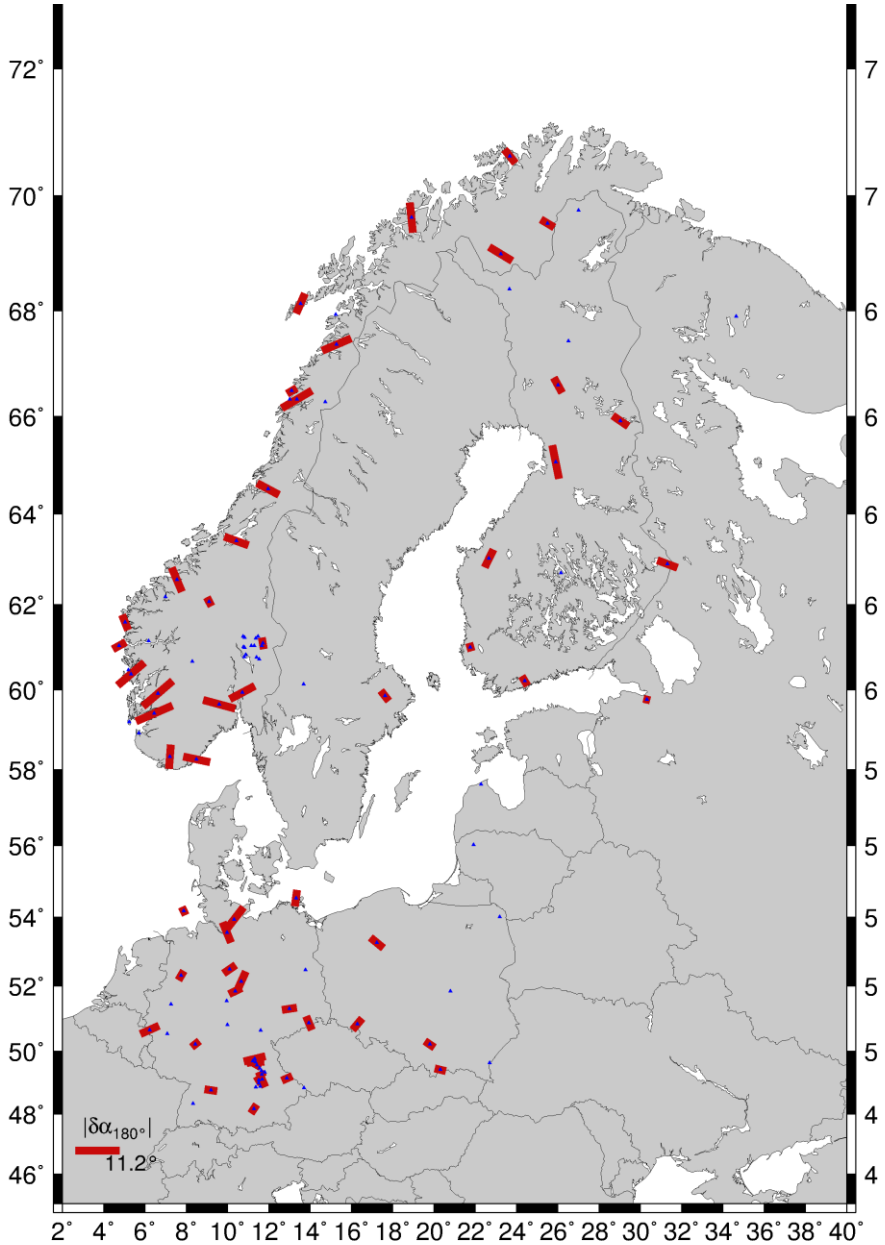

Figure 22. Fast directions of azimuthal anisotropy at the permanent stations in Norway and surrounding countries, estimated from the phase of 180° term at high frequencies. At the stations of NNSN is not observed any strong dependence of the fast direction on the frequency. At the stations of the German Seismic Network, the frequency dependence of the fast direction is more pronounced.

5.2 Magnitude scale for earthquakes along the mid-Atlantic Ridges in Offshore Norway

by Won-Young Kim, Lamont-Doherty Earth Observatory of Columbia University

The main objectives of this study are to determine the amplitude attenuation of Pn and Sn phases in the northern Atlantic region to establish a regional magnitude scale that is robust despite complex wave propagation paths in the ocean basins and fracture zones. The amplitude decay of regional phases (Pn, Pg, Sn, and Lg) with distance can be described as a power-law distance dependence. Some Pn and Sn phases excited at the source on the mid-Atlantic ridge are passing through additional mid-Atlantic ridge segment. For example, Pn phase generated by an event on the Jan Mayan ridge propagates along oceanic crust underneath the Norwegian Sea, then encounters the Knipovich segment (Nansen fracture zone) of mid-Atlantic ridge before it arrives at station KBS on the Svalbard. In such cases, the amplitude attenuation must be more severe than single path due to scattering loss of Pn or Sn phase amplitudes.

A total of 986 Pn and 600 Sn observations from 132 earthquakes that occurred along the northern mid-Atlantic ridges recorded at 19 stations of 14 NNSN (Norwegian National Seismic Network) and five GSN stations in Greenland (Figure 23). These earthquakes are selected from the GCMT (Global Centroid Moment Tensor) catalog during 2000-2015. The moment magnitudes of the selected events are used as reference to determine amplitude distance curves for Pn and Sn phases in the region. Observed RMS (root-mean-squared) amplitudes in micron/s are normalized by the moment magnitude (Mw) of each event and are plotted in Figure 24 against distance.

Station correction, amplitude distance curve which consists of frequency dependent attenuation and geometrical spreading of amplitude, are solved by damped least-square inversion following the approach by Sereno (1990), Jenkins et al. (1998), and Hicks et al. (2004). We obtained a robust magnitude scale for earthquakes that occur along the northern mid-Atlantic ridges using Pn and Sn in the distance ranges from 200 km to 2,000 km. Using the new mb(Pn) magnitude scale, we obtained the magnitudes that are comparable to the Mw from GCMT catalog with scatter of only 0.05 m.u. (Figure 25). A key to make the mb(Pn) scale applicable to wide range of earthquake size and regions is to generalize the source-specific correction terms that are necessary due to diverse wave propagation paths involved with the mid-Atlantic ridge earthquakes.

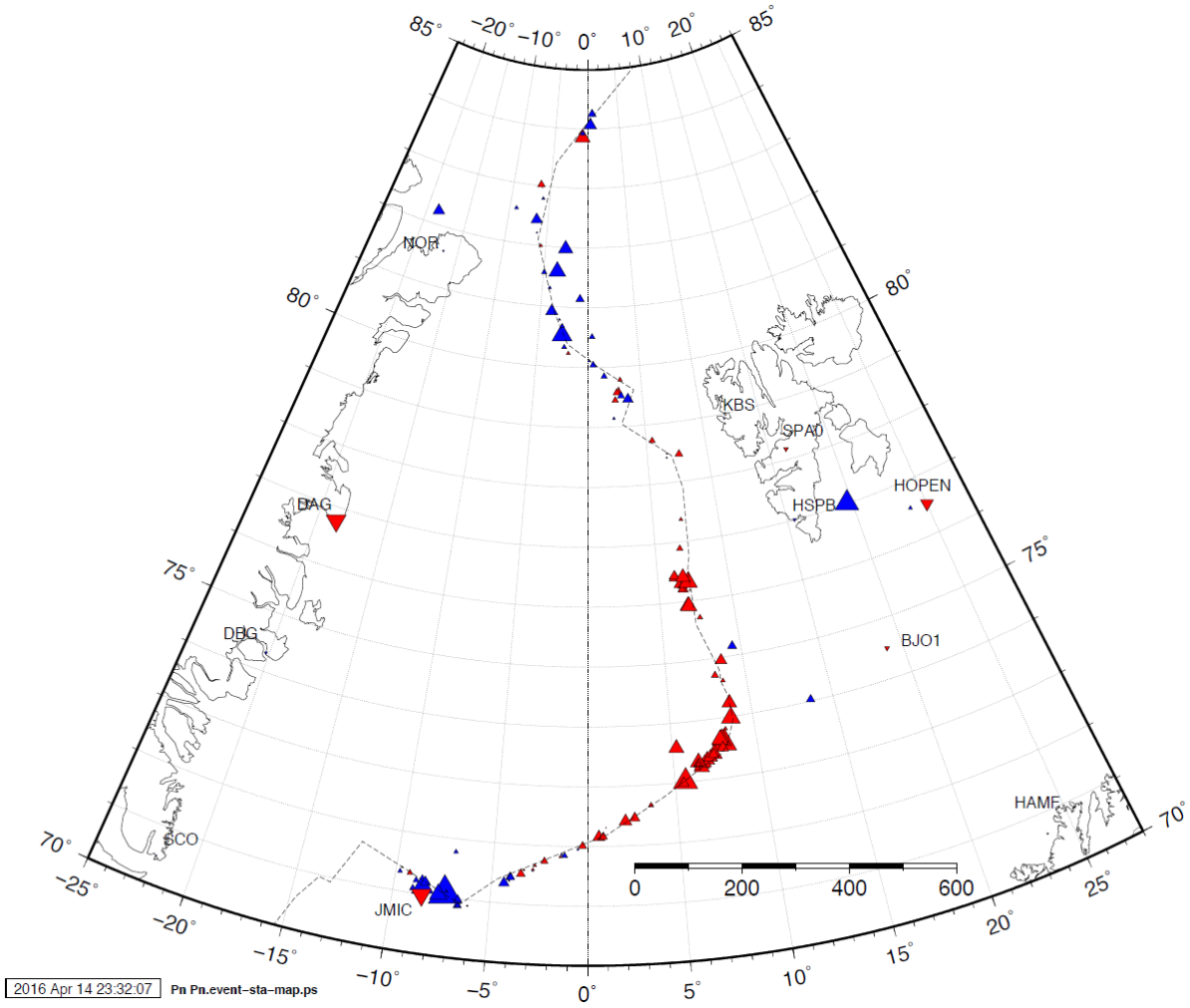

Figure 23. Results of the Pn amplitude inversion for amplitude attenuation parameters (α, *a* & *b*), station corrections, and event correction terms. Stations with positive corrections (e.g., DAG=0.17, JMIC=0.18 & HOPEN=0.11) are plotted with red inverted triangles, whereas the negative station corrections are plotted with blue inverted triangles. The symbol size is proportional to the corrections. Similarly, events with positive corrections plotted with red triangles which are mostly on Mohns Ridge, and lower half of Kinipovich Ridge, whereas the negative corrections (blue triangles) are mostly on Jan Mayen transform fault region and Nansen fracture zone west and northwest of Svalbard. The corrections are added to the magnitude determination, and hence, the negative corrections indicated large measured amplitude than other events.

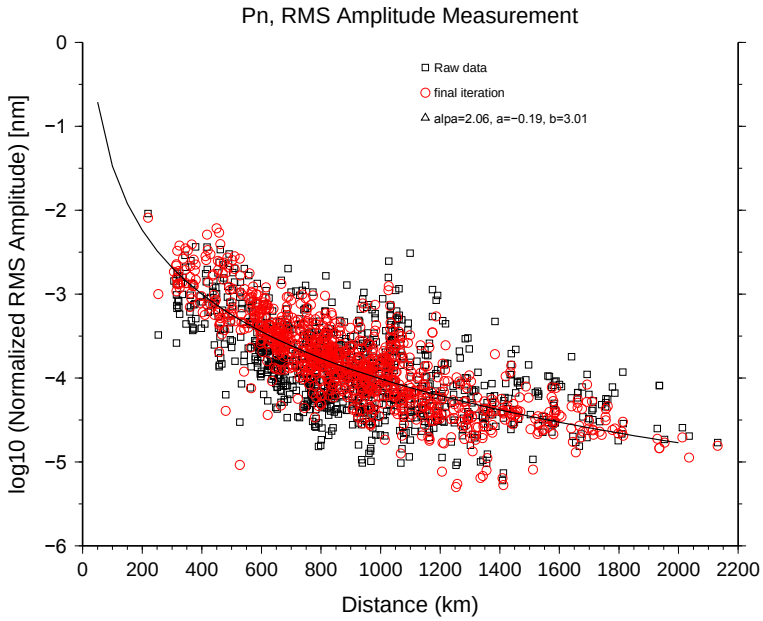

Figure 24. 986 $\log_{10}$ (RMS amplitude) of Pn phases are plotted against distance (black circles). Amplitudes are normalized by their moment magnitude. Amplitudes after the inversion are plotted with red circles, and the amplitude-distance obtained from the inversion is superposed with the amplitudes. The curve is parameterized by $\alpha = 2.06$, $a = -0.19$ f and $b = 3.01$.

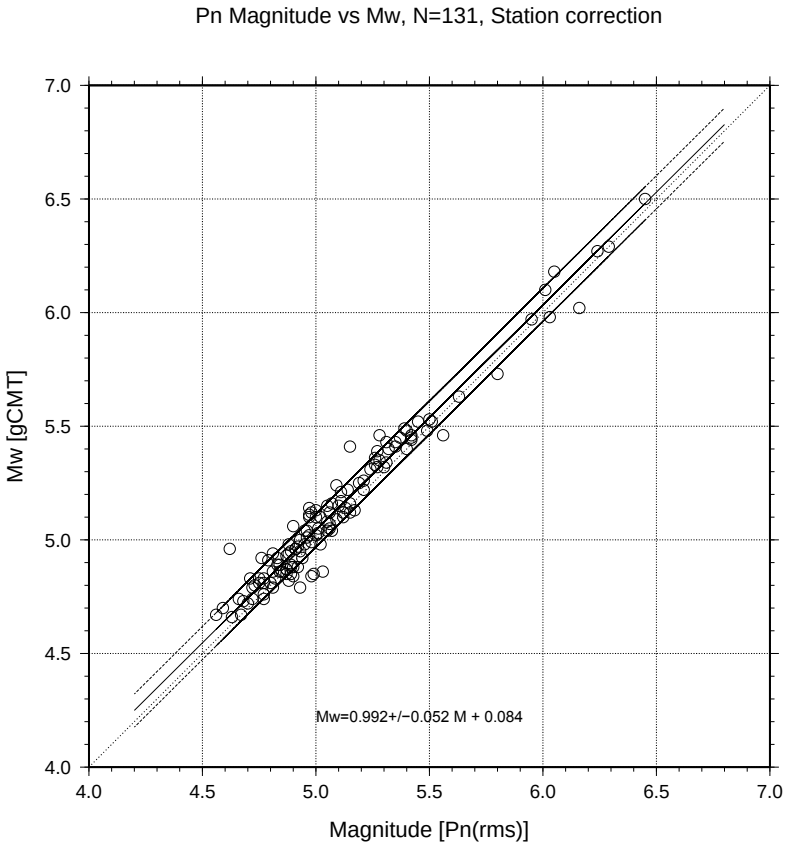

Figure 25. Result of the inversion indicated that the new magnitude obtained from Pn phases M(Pn), using the measured RMS amplitudes (in 1-4 Hz band) are consistent with original event moment magnitude with Mw = 0.992±0.052 mb(Pn) + 0.084. Notice that scatters are only 0.05 magnitude units.

5.3 Development of a 3-D velocity model for Norway

by Ilma Janutyte, NORSAR

The aim of this study is to develop the 3-D crustal model for the territory of Norway both on-shore and off-shore. The 3-D model would help to locate the seismic events in Norway with higher precision. During the last year we upgraded the 3-D crustal velocity model for the southern part of Norway, and developed new velocity models for the territory of Nordland, northern Norway, and Finnmark, the northernmost part of Norway (Figure 26).

The workflow was divided into two steps: 1) development of the optimal 1-D velocity models for southern Norway and Nordland, while for Finnmark we used the FESCAN (Mykkeltveit and Ringdal, 1981) 1-D velocity model as optimal one, and 2) development of the 3-D velocity models. The final goal is to merge the models into one for entire Norway.

The optimal 1-D velocity models were obtained using the VELEST program (Kissling et al., 1994), which is implemented into the SEISAN program package (Ottemoller et al., 2014). The obtained optimal 1-D velocity models extend from the surface down to 80 km deep and consist of several layers of different but constant seismic velocities. To develop the velocity model for the southern Norway we used a dataset of 175 local seismic events recorded at 105 stations, for Nordland we used a dataset of 100 events recorded at 29 stations, and for Finnmark we used a dataset of 113 events recorded at 55 seismic stations (Figure 27).

Before implementing the 1-D velocity models into the FMTOMO program (Rawlinson and Sambridge, 2005), which was used for the 3-D inversion, the 1-D velocity model was transformed into the two layer models with gradient increase in velocities with depth. The upper layer was set from the surface down to the depth of the Moho boundary, and the lower layer was from the Moho down to 80 km depth. The synthetic checkerboard tests with the current configuration of sources and receivers were used to check the resolution in each territory separately. Beneath the areas spanned by the seismic networks of each study area the resolution is reasonably good down to 35-40 km depths. The 3-D inversion results show velocity perturbations up to ±0.4 km/s for southern Norway and Finnmark, and up to ±0.6 km/s for Nordland, as compared to the reference velocity models. The higher velocity contrast in Nordland might be related to the more complex geological conditions compared to the other parts of Norway. The obtained results were compared to the results obtained from earlier studies.

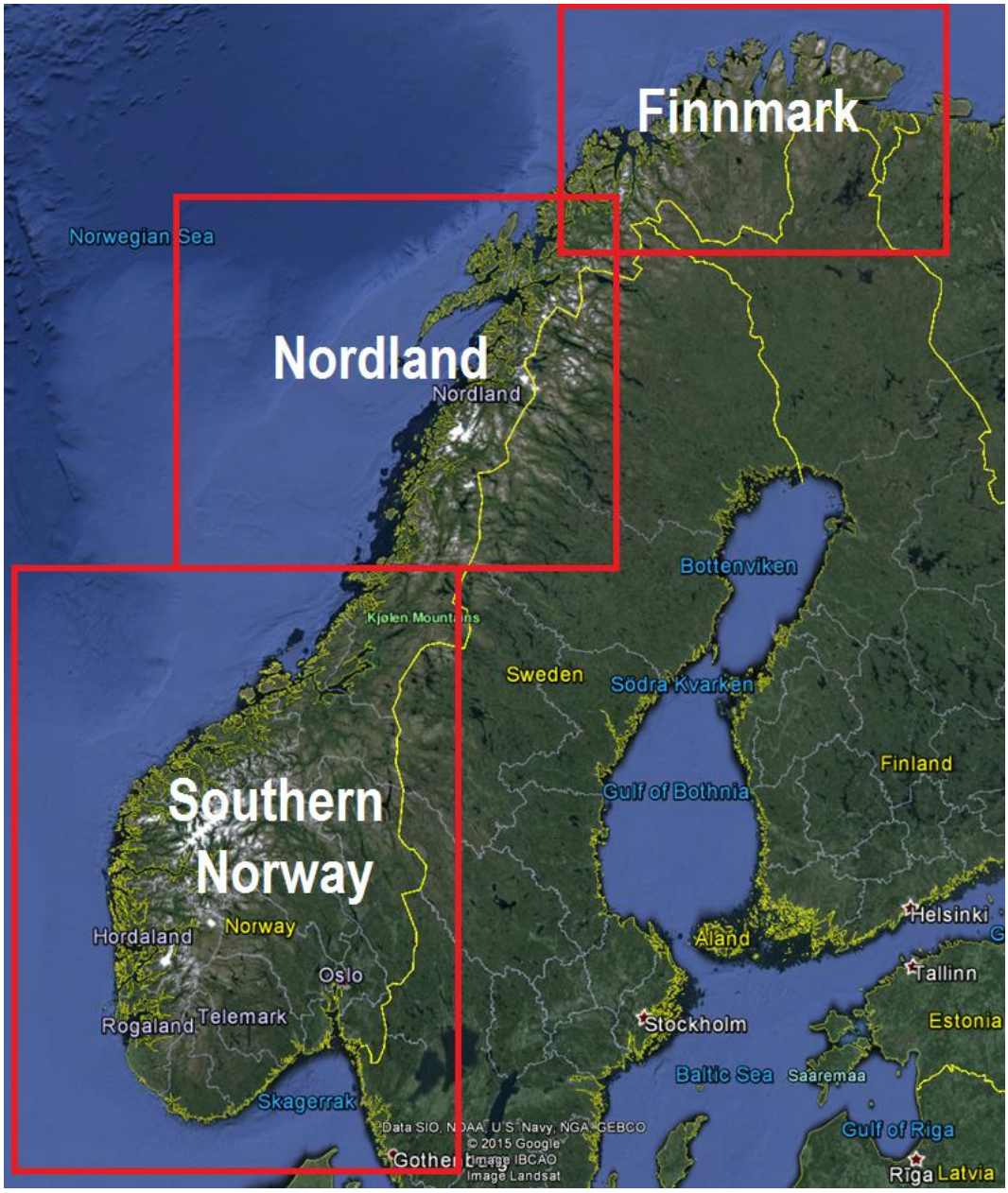

Figure 26 Areas of Norway with developed 3-D crustal velocity models.

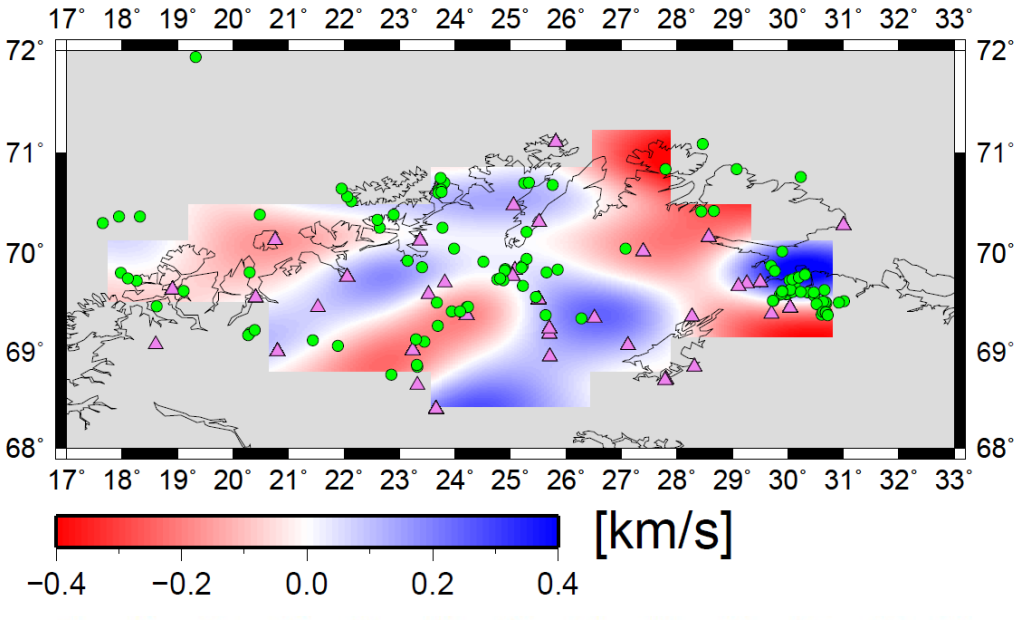
17° 18° 19° 20° 21° 22° 23° 24° 25° 26° 27° 28° 29° 30° 31° 32° 33°
72° 71° 70° 69° 68°
[km/s]
−0.4 −0.2 0.0 0.2 0.4

a)

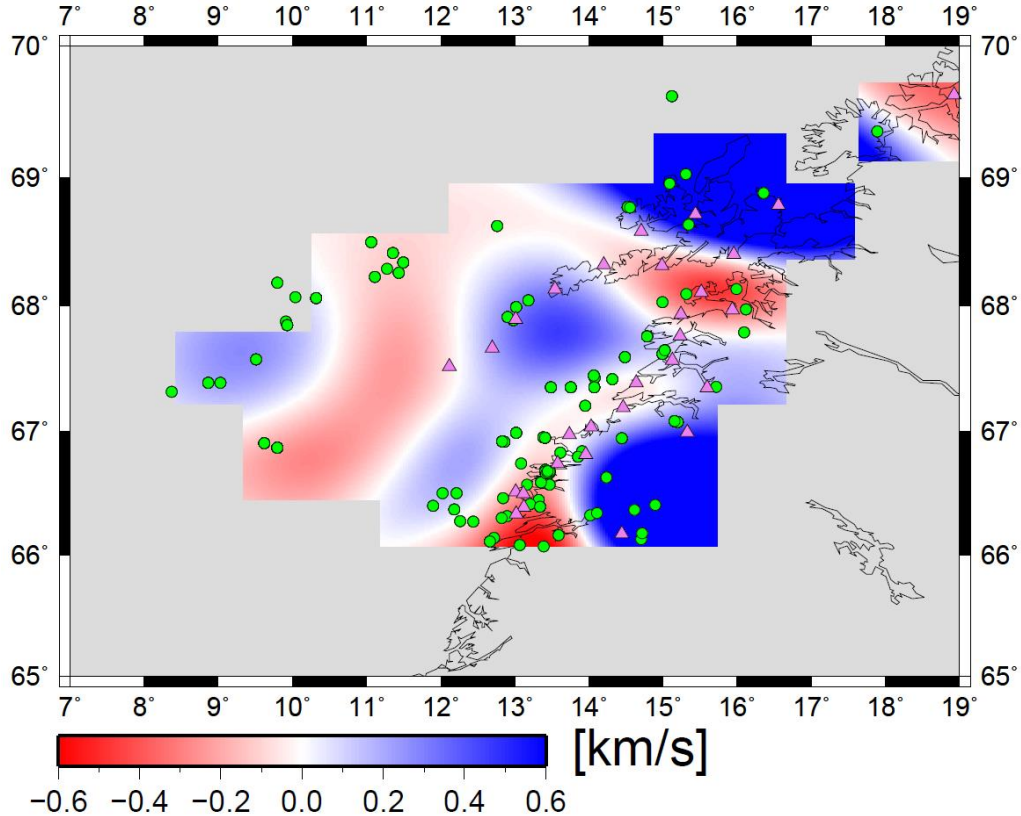
7° 8° 9° 10° 11° 12° 13° 14° 15° 16° 17° 18° 19°
70° 69° 68° 67° 66° 65°
[km/s]
−0.6 −0.4 −0.2 0.0 0.2 0.4 0.6

b)

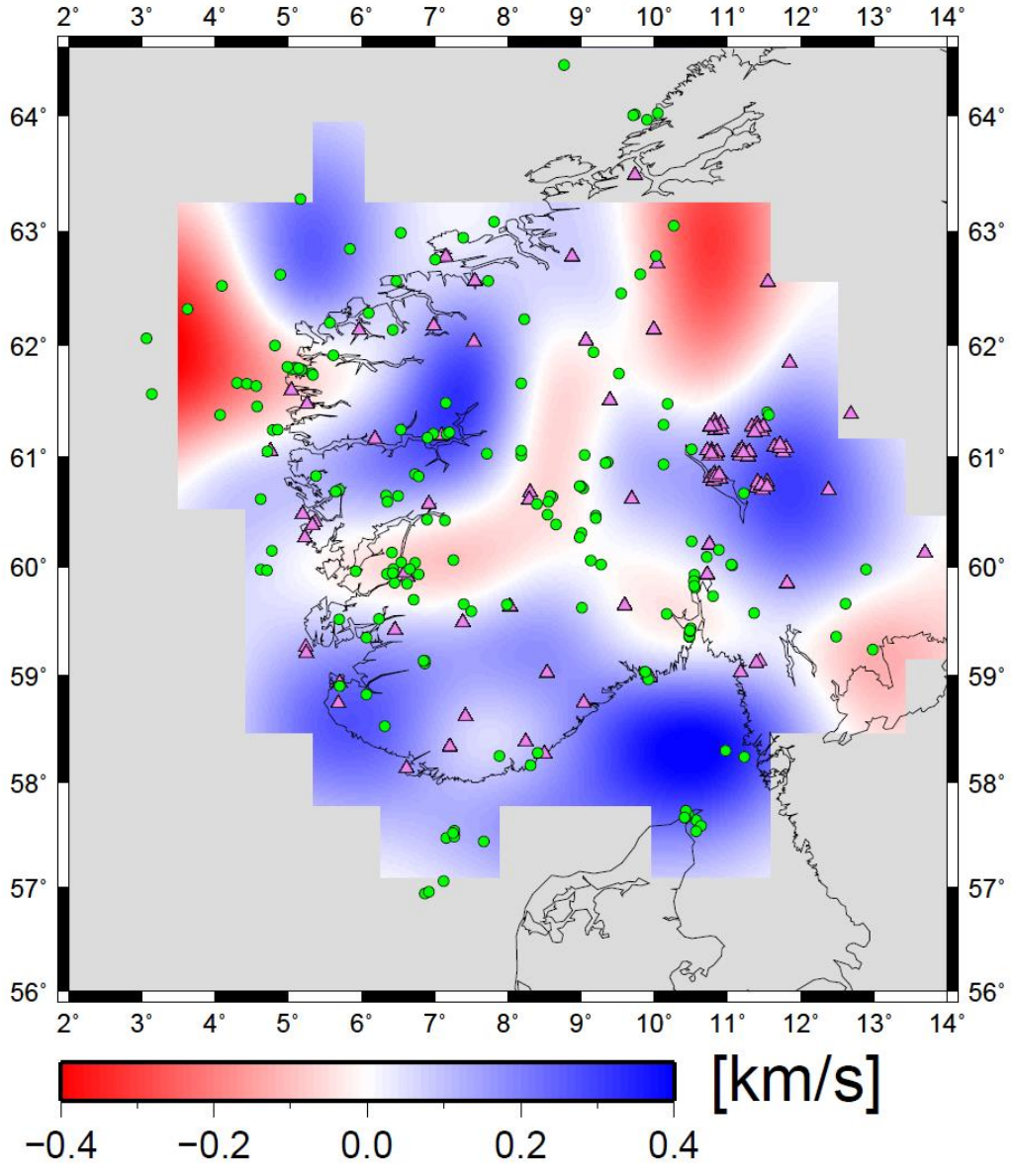

c)

Figure 27 Horizontal slice at 10 depth of the 3-D velocity models developed for the territories of Finnmark (a), Nordland (b) and southern Norway (c) (see Fig. 1). Triangles mark the seismic stations, green circle mark the epicenters of earthquakes. Red and blue areas indicate the resolved seismic velocities lower or higher, respectively, compared to the reference velocity models. The areas with poor resolution are colored in grey.

5.4 Testing of a method for distinguishing between earthquakes and explosions

by Ilma Janutyte, NORSAR

We have started experiments with a method which can help to objectively distinguish between earthquakes (EQs) and explosions. The method was first developed at the Institute of Seismology, University of Helsinki, Helsinki, Finland (Kortstrom et al., 2016), and is successfully used there by their analysts.

The idea of the method is to calculate spectral parameters from the seismograms and compare them with the spectral models developed for EQs and explosions, respectively. The workflow is divided into several steps: 1) the event seismogram is divided into four equal time windows of the length depending on the time difference between P and S waves, 2) the seismogram is filtered with 20 narrow band filters covering range from 1 to 41 Hz, 3) the short term averages (STA) are calculated for each window with different filters, so the set of 80 spectral parameters are obtained, 4) the set of parameters are compared to the reference models, which must be developed beforehand, and finally 5) the prediction for the event is presented. For steps 1-3 we wrote a script in ObsPy, while steps 4-5 were conducted using the SVM^{light} (Joachims, 1999).

The method requires reference spectral earthquake and explosion models for each station. As a first test we developed reference spectral models for two NNSN seismic stations, HYA and FOO. Using 121 events of the NNSN bulletin, labelled as earthquakes or explosions, we obtained models for station HYA (Figure 28), for which validation was performed with 125 different events with 92 % of correct predictions. For station FOO we used 64 events for obtaining the earthquake and explosion spectral models, and validation was performed with 65 different events with 98 % of correct predictions. We also performed a test for 58 events which were recorded in both seismic stations, HYA and FOO. The prediction results are presented in Figure 29. These initial results are encouraging, but studies of larger datasets, including more stations, are needed to make the method generally applicable as a tool for distinguishing between earthquakes and explosions in our region.

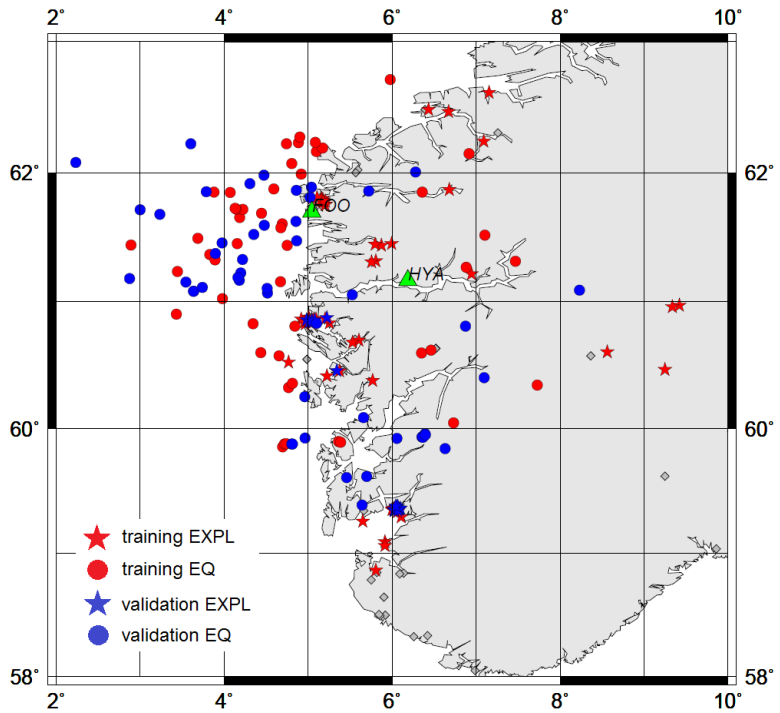

Figure 28 Seismic events used to develop and verify spectral models for station HYA. The seismic events are marked as circles and stars, and seismic stations HYA and FOO are marked as green triangles.

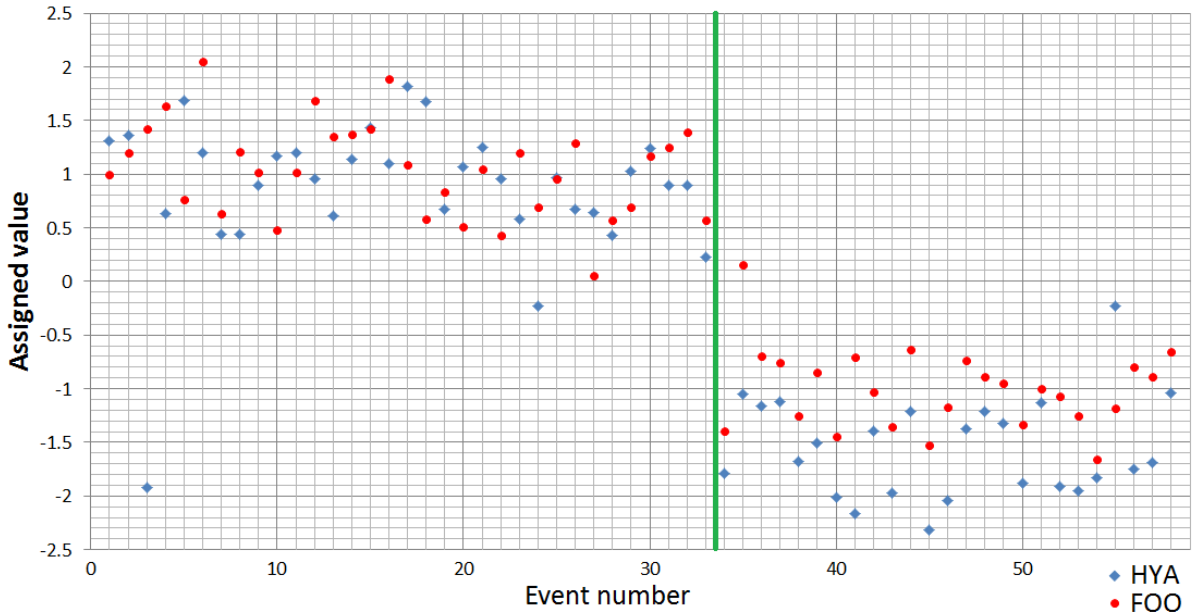

Figure 29 Results obtained with common dataset for seismic stations HYA and FOO. Green line indicates the boundary between EQs and explosions in the dataset (33 EQs and 25 explosions). Red dots and blue diamonds represent stations FOO and HYA, respectively. The values indicate the prediction: the more positive value, the more the event is EQ-like, while the more negative, the more explosion-like.

5.5 Relocating seismicity using a Bayesian hierarchical multiple event location algorithm

by Steven J. Gibbons, NORSAR

Many recent studies have demonstrated that multiple-event location algorithms can provide far more accurate estimates for the location of seismicity than classical single-event location procedures. We have demonstrated that a far better constrained image of seismicity on the mid-Ocean ridge in the Arctic can be obtained using the Bayesian hierarchical multiple event location algorithm Bayesloc (Myers et al., 2007, 2009) which results in implicit corrections to the applied velocity model. We have started to explore the applicability of Bayesloc to seismicity offshore of southern Norway. The results are more difficult to evaluate than for the mid-Atlantic ridge because the seismicity is more diffuse and is not as limited to well-mapped-out tectonic structures. However, preliminary results (Figure 30) are highly promising with the simultaneously inverted seismicity (panel b) showing more spatially consistent deviations from the applied velocity model than the corresponding single-event location estimates (panel a). We can exploit the long history of recordings from stations in southern Norway and in the UK, even providing constraints on recent seismicity from historical events that were well-constrained by temporary deployments (e.g. Weidle et al., 2010). We intend to explore further the ability of Bayesian algorithms to identify clusters of seismicity and to estimate empirical correction terms to velocity models used in routine event location procedures.

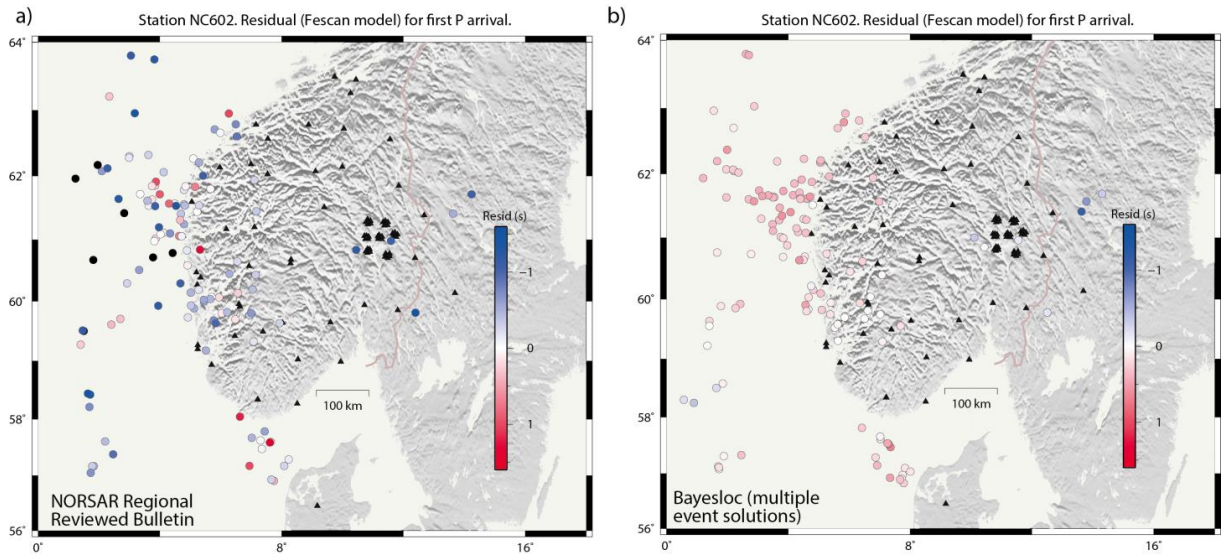

Figure 30. Time residual in seconds for the initial regional P-arrivals at the NC602 station of the NORSAR array, relative to the Fescan velocity model (see Mykkeltveit and Ringdal, 1981) for (a) NORSAR reviewed event locations and (b) the preliminary Bayesloc solutions.

6 Publications and presentations of NNSN data during 2015

Data collected on Norwegian seismic stations are made available through the Internet and is provided on request to interested parties. Therefore it is difficult to get a comprehensive overview on the use and all publication based on Norwegian data. The following reference list shows publications and presentations of UiB and NORSAR scientists for the reporting period, based on data of NNSN and NORSAR stations.

6.1 Publications

Antonovskaya, G., Konechnaya, Y., Kremenetskaya, E. O., Asming, V., Kværna, T., Schweitzer, J., Ringdal, F.: Enhanced earthquake monitoring in the European Arctic, Polar Science, **9**, 158-167, 2015, doi: 10.1016/j.polar.2014.08.003

Atakan, K., Bjerrum, L.W., Bungum, H., Dehls, J.F., Kaynia, A.M., Keers, H., Kierulf, H.P., Kværna, T., Langeland, T., Lindholm, C.D., Maupin, V., Ottemöller, L., Sørensen, M.B. and Yuen, M.Y. (2015). The European Plate Observing System and the Arctic, Arctic, 68 (S1), doi:10.14430/arctic4446.

Junek, W. N., Kværna, T., Pirli, M., Schweitzer, J., Harris, D. B., Dodge, D. A., Woods, M. T.: Inferring aftershock properties and tectonic structure using empirical signal detectors, Pure Appl. Geophys., **172**, 359-373, 2015, doi: 10.1007/s00024-014-0938-0

Köhler, A., Nuth, C., Schweitzer, J., Weidle, C., Gibbons, S. J.: Regional passive seismic monitoring reveals Dynamic glacier activity on Spitsbergen, Svalbard Polar Research, **34**, 26178, 19 pp., doi: 10.3402/polar.v34.26178

Schweitzer, J., Fyen, J., Roth, M.: NORSAR's modernized, large-aperture broadband array NOA, Norway Vestnik NNC RK Bulletin, ISSN 1729-7516, **4(64)**, 1-14, 2015

6.1 Master degree thesis, UiB

M. Johnsen: Seismic hazard due to large earthqukes in Norway, MSc thesis, Dept. of Earth Science, UiB, June 2016.

6.2 Reports

Veim, M. K. Revision of station coordinates. NNSN Tech. Rep. 28, Department of Earth Science, University of Bergen, 2015.

Strømme, M.L. Spectrogram function for routine processing. NNSN Tech. Rep.29, Department of Earth Science, University of Bergen, 2015.

6.3 Oral presentations

Janutyte, I., Schweitzer, J., Gibbons, S. J., Ottemöller, L., Kværna, T.: 3-D crustal model for Norway, Nordic Seismological Seminar, Bornholm, October 2015

Konechnaya, Y., Antonovskaya, G., Kremenetskaya, E., Vinogradov, Y., Kvaerna, T., Schweitzer, J., Ivanova, E.: Seismic monitoring in the European Arctic: first results of a Cooperative project 26th General Assembly IUGG, Prague, 22 June – 2 July 2015

Kværna, T., Gibbons, S. J., Schweitzer, J.: The October 11, 2010 Novaya Zemlya Earthquake: Implications for Velocity Models and Regional Event Location NORRUSS GEOPROC Project, 2nd Workshop, Arkhangelsk, 4 – 8 May 2015

Odden, G., Minakov, A., Schweitzer, J.: The lower crust and upper mantle beneath Svalbard and the Western Barents Sea: evidence from combined active-source and array seismology 7th International Conference on Arctic Margins, Trondheim, 2 – 5 June 2015

Mäntyniemi P. and M.B. Sørensen: A joint Nordic effort to compile a modern macroseismic map on the strong earthquake of 23rd October 1904. Presentation at the 46th Nordic Seismology Seminar, Bornholm, 30. Sep. – 2. Oct. 2015.

Michalek J., I. Janutyte, L. Ottemöller, C. Lindholm (2015). Seismicity of the Nordland area, Norway. 46th Nordic Seismology Seminar, Bornholm, Denmark (30.9.-2.10.2015), presentation.

Ottemöller, L. With and against seismic noise, Nordic Seismological Seminar, Bornholm, October 2015.

Roth, M.: NORSAR stations – current status, Nordic Seismological Seminar, Bornholm, October 2015

Schweitzer, J.: 3D Crustal Models of the Barents Sea – Putting the Puzzle Together Seminar at CEED, University of Oslo: “From Barents to Bouvet – Celebrating Jan Inge Faleide”; 9th April 2015 (invited talk)

Schweitzer, J.: Regional and international event locations in the European Arctic NORRUSS GEOPROC Project, 2nd Workshop, Arkhangelsk, 4 – 8 May 2015

Schweitzer, J.: Source Characteristics of the 11 October 2010 Novaya Zemlya Earthquake NORRUSS GEOPROC Project, 2nd Workshop, Arkhangelsk, 4 – 8 May 2015

Schweitzer, J.: Regionalized models for the location of seismic events in the European Arctic NORRUSS GEOPROC Project, 3rd Workshop, NORSAR, 19 – 23 October 2015

Sørensen, M.B.: What is the link between seismicity and seismic hazard? Examples from Norway and abroad. Presentation at GEO partner day, 12. Feb. 2015.

Sørensen, M.B.: Geofare forskning ved GEO, UiB. Presentation at SAK geofare seminar, Åndalsnes, 19-21 October 2015.

6.4 Poster presentations

Celli, N. L., Schweitzer, J., Fyen, J.: The NORSAR Long Period Detector: a tool for surface waves detection and parameter extraction 26th General Assembly IUGG, Prague, 22 June – 2 July 2015 (poster)

Gibbons, S. J., Schweitzer, J., Roth, M., Kværna, T.: Improved detection and parameter estimation for regional S-phases using the fully 3-component ARCES array, CTBT: Science and Technology 2015 Conference (SnT2015), Vienna, 22 - 26 June 2015 (poster)

Gibbons, S. J., Kværna, T., Näsholm, S. P.: Searchlight Correlation Detectors: Optimal Seismic Monitoring Using Regional and Global Networks, CTBT: Science and Technology 2015 Conference (SnT2015), Vienna, 22 - 26 June 2015 (poster)

Gibbons, S. J., Schweitzer, J., Roth, M., Kværna, T.: Improved detection and parameter estimation for regional S-phases using the fully 3-component ARCES array 26th General Assembly IUGG, Prague, 22 June – 2 July 2015 (poster)

Janutyte, I., Storheim, B. M., Paulsen, B., Stromme, M. L., Schweitzer, J. + Gibbons, S. J., Ottemöller, L., Lindholm, C., Kvaerna, T.: 3-D crustal velocity model for Norway 12. EGU General Assembly, Vienna, April 2015 (poster)

Konechnaya, Y., Vaganova, N., Asming, V., Kvaerna, T., Gibbons, S. J., Schweitzer, J.: Location of seismic events in the Eastern Barents Sea region 26th General Assembly IUGG, Prague, 22 June – 2 July 2015 (poster)

Köhler, A., Nuth, C., Weidle, C., Schweitzer, J., Kohler, J., Buscaino, G.: Towards quantification of glacier dynamic ice loss trough passive seismic monitoring AGU Fall Meeting 2015, 14-18 December, San Francisco, California. Paper Number: C43B-0802 (poster)

Michalek J., L. Ottemöller (2015). Seismicity of the Lofoten area, Norway. 26th IUGG General Assembly 2015, Prague, Czech Republic (22.6.-2.7.2015), poster.

Ohrnberger, M., Hammer, C., Spieler, M., Schweitzer, J.: Glacier seismicity in the vicinity of SPITS monitoring array 26th General Assembly IUGG, Prague, 22 June – 2 July 2015 (poster)

Ritter, J. R. R., Roy, C., Schweitzer, J.: On the improvement of SKS splitting measurements by the Simultaneous Inversion of Multiple Waveforms (SIMW)
AGU, Fall Meeting 2015, 14-18 December, San Francisco, California. Paper Number: DI21A-2599 (poster)

Roth, M., Fyen, J., Kværna, T., Gibbons, S. J.: The all three-component broadband seismic array ARCES/PS28, CTBT: Science and Technology 2015 Conference (SnT2015), Vienna, 22 - 26 June 2015 (poster)

7 References

Alsaker A., Kvamme, L.B., Hansen, R.A., Dahle, A. and Bungum, H. (1991): The ML scale in Norway. *Bull. Seism. Soc. Am.*, Vol. **81**, No. 2, pp.379-398.

Andersen K. (1987): Local seismicity and volcanism in the Jan Mayen area. McS., Department of geosciences, University of Bergen.

Atakan,K., Lindholm,C.D., and Havskov,J. 1994. Earthquake swarm in Steigen, northern Norway: An unusual example of intraplate seismicity. *Terra Nova* **6**, 180-194.

Brune J.N. (1970): Tectonic stress and spectra of seismic shear waves. *Journal of Geophysical Research*, **75**, 4997-5009.

Cristiano,L.,Meier, T., Keers, H., Krüger, F., Weidle, C. Teleseismic P-wave polarization analysis at the Gräfenberg array, in preparation.

Grünthal, G. (1998): "European Macroseismic Scale 1998". Cahiers du Centre Européen de Géodynamique et de Séismologie Volume 15, Luxembourg.

Havskov J., and Bungum, H. (1987): Source parameters for earthquakes in the northern North Sea. *Norsk Geologisk Tidskrift*,Vol.**67**, pp 51-58.

Havskov, J. and Ottemöller, L. (1999): SEISAN earthquake analysis software. *Seism. Res. Letters*, Vol. 70, pp. 532-534.

Havskov, J. and Ottemöller, L. (2001): SEISAN: The earthquake analysis software. Manual for SEISAN v. 8.0, Department of Earth Science, University of Bergen, Norway.

Havskov, J. and Sørensen, M.B. (2006): New coda magnitude scales for mainland Norway and the Jan mayen region. *NNSN Technical report no. 19.*

Hicks, E.C., H. Bungum and C. Lindholm, Seismic activity, inferred crustal stresses and seismotectonics in the Rana region, Northern Norway, *Quaternary Science Reviews 19*, 1423-1436, 2000).

Hicks, E.C., T. Kværna, S. Mykkeltveit, J. Schweitzer, and F. Ringdal (2004). Travel-times and attenuation relations for regional phases in the Barents Sea region, *Pure appl. geophys*. **161**, 1–19.

Hicks, E.C. and L. Ottemöller, The M_L Stord/Bømlo, southwestern Norway, earthquake of August 12, 2000, *Norsk Geologisk Tidsskrift* (Norwegian Journal of Geology), 81, 293-304, 2002.

Jenkins, R.D., T.J. Sereno, and D.A. Brumbaugh (1998). Regional attenuation at PIDC stations and the transportability of the S/P discriminant, *AFRL-VS-HA-TR-98-0046*, Science Applications International Corporation, San Diego, CA., USA.

Joachims, T.: Making large-Scale SVM Learning Practical. Advances in Kernel Methods - Support Vector Learning. Schölkopf, B., Burges, C,. and Smola, A. (eds.), MIT-Press, 1999

Jurkevics, A. (1988). Polarization analysis of three-component array data. Bull. Seism. Soc. Amer., 78, (5), 1725-1743.

Kanamori, H. (1977): The energy release in great earthquakes. *Journal of Geophysicsl Research* 82; 20, pp. 2981-2987.

Karnik, V., Kondorskaya, N.V., Riznichenko, Y. V., Savarensky, Y. F., Solovev, S.L., Shebalin, N.V., Vanek, J. and Zatopek, A. (1962): Standardisation of the earthquake magnitude scales. *Studia Geophys. et Geod*., Vol. **6**, pp. 41-48.

Kennett, B.L.N. and Engdahl, E.R. (1991): Traveltimes for global earthquake location and phase identification. *Geophys. J. Int*., Vol. **105**, pp. 429-465.

Kissling, E., W.L. Ellsworth, D. Eberhart-Phillips and U. Kradolfer (1994). Initial reference models in local earthquake tomography. *J. Geophys. Res*., **99**, 19, 635-19, 646.

Kortstrom, J., Uski, M., and Tiira, T.: Automatic classification of seismic events within a regional seismograph network. Computers and Geosciences, 87, 22-30, 2016, doi: 10.1016/j.cageo.2015.11.006

Kradolfer, U. (1996): AuroDRM – The First Five Years. *Seismological Research Letters,* vol. 67, no. 4, 30-33.

Lienert, B.R. and Havskov, J. (1995): HYPOCENTER 3.2 A computer program for locating earthquakes locally, regionally and globally. *Seismological Research Letters*, Vol. **66**, 26-36.

Mayeda, K., A. Hofstetter, J. L. O'Boyle and W.R. Walter (2003). Stable and Transportable Regional Magnitudes Based on Coda-Derived Moment-Rate Spectra. *Bull. Seism. Soc. Am,*. **93** , 224-239.

Moreno, B, Ottemöller, L., Havskov, J. and Olesen, K.A. (2002): Seisweb: A Client-Server-Architecture-Based Interactive Processing Tool for Earthquake Analysis. *Seism. Res. Letters.* Vol.73, No.1.

Myers, S. C., Johannesson, G., and Hanley, W. (2007), A Bayesian hierarchical method for multiple-event seismic location, *Geophysical Journal International*, 171, 1049-1063.

Myers, S. C., Johannesson, G., and Hanley, W. (2009), Incorporation of probabilistic seismic phase labels into a Bayesian multiple-event seismic locator, *Geophysical Journal International*, 177, 277-289.

Mykkeltveit, S., and Ringdal, F.: Phase identification and event location at regional distances using small-aperture array data. In 'Idendification of seuismic sources – Earthquake or underground explosions', p. 467-481, Husebye and Mykkeltveit (eds.) Reidel Publishing Company, 1981

Niazi, M. (1966). Corrections to apparent azimuths and travel-time residuals for a dipping Mohorovicic discontinuity. Bull. Seismol. Soc. Am., 56, 491-509.

Ottemöller, L. (1995): Explosion filtering for Scandinavia. *Technical Report* No. **2**, Institute of Solid Earth Physics, University of Bergen, Norway.

Ottemoller, L., Voss, P., and Havskov, J.: SEISAN EARTHQUAKE ANALYSIS SOFTWARE FOR WINDOWS, SOLARIS, LINUX and MACOSX , 2014

Pirli, M., Schweitzer, J., Ottemöller, L., Raeesi, M., Mjelde, R., Atakan, K., Guterch, A., Gibbons, S. J., Paulsen, B., Debski, W., Wiejacz, P. and Kvaerna T. Preliminary Analysis of the 21 February 2008 Svalbard (Norway) Seismic Sequence, Seismological Research Letters, 81: 63-75, 2010.

Rawlinson, N. and M. Sambridge (2005). The fast marching method: an effective tool for tomographic imaging and tracking multiple phases in complex layered media. *Exploration Geophysics*, **36** (4), 341-350.

Roy, C. & Ritter, J.R.R.: Complex deep seismic anisotropy below the Scandinavian mountains. J. Seismo., 17, 361-384, , 2013.

Sato, H., M. C. Fehler and T. Maeda (2009). Seismic wave propagation and scattering in the heterogeneous Earth. Chapter 2.4, Scattering of high-frequency seismic waves. *Springer-Verlag Berlin Heidelberg*. 19-40.

Schweitzer, J. The 21 July 2011 earthquake in Hedmark, Southern Norway Semiannual Technical Summary, 1 January – 30 June 2011, NORSAR Scientific Report, 2–2011, 44-50, Kjeller, Norway, 2011.

Schulte-Pelkum, V., G. Masters & P. Shearer (2001). Upper mantle anisotropy from long period P wave polarization. J. Geophys. Res., 106, (B10), 21917-21934.

Sereno, T. J. (1990). Attenuation of regional seismic phases in Fennoscandia and estimates of arrival time and azimuth uncertainty using data recorded by regional arrays, *Tech. Rep. SAIC-90/1472*, Science Applications International Corp., San Diego, CA., USA.

Sørensen, M.B., Ottemöller, L., Havskov, J., and Atakan, K., Hellevang, B., Pedersen, R.B. 2007. Tectonic processes in the Jan Mayen Fracture Zone based on earthquake occurrence and bathymetry. *Bulletin of the Seismological Society of America*, Vol.**97** No.3, 772-779, doi: 10.1785/0120060025.

Veith K.F., and Clawson, G.E. (1972): Magnitude from short-period P-wave data. *Bull. Seism. Soc. Am.*, Vol. **62**, pp.435-452.

Waldhauser F. and W.L. Ellsworth, A double-difference earthquake location algorithm: Method and application to the northern Hayward fault, *Bull. Seism. Soc. Am.*, 90, 1353-1368, 2000.

Weidle, C., Maupin, V., Ritter, J., Kværna, T., Schweitzer, J., Balling, N., Thybo, H., Faleide, J. I., and Wenzel, F. (2004), MAGNUS--A Seismological Broadband Experiment to Resolve

Crustal and Upper Mantle Structure beneath the Southern Scandes Mountains in Norway, *Seismological Research Letters*, **81**, 76-84.

Westre S. (1975): Richter's lokale magnitude og total signal varighet for lokale jordskjelv på Jan Mayen. *Cand. real thesis*., Seismological Observatory, University of Bergen, Norway.